Reggeon calculus as a low-order perturbation theory for the Pomeron*

Carleton DeTar[1]
Laboratory for Nuclear Science and Department of Physics,
Massachusetts Institute of Technology, Cambridge, Massachusetts 02139
(Received 5 August 1974)

We review the foundations of the Gribov Reggeon calculus with an emphasis on the relationship between the energy-plane and J-plane descriptions of the diagrams of the calculus. The question of the "large-rapidity-gap cutoff" for the Pomeron and the problem of signature are treated in more detail than in the traditional approach to the calculus. Except for some slight differences, the main results agree with Gribov's original formulation. We advocate the use of the Reggeon calculus as a refinement on the contemporary "two-component" model for the Pomeron and collect some formulas useful for phenomenological applications.

I. INTRODUCTION

Ever since the high-energy behavior of cross sections was described in terms of a leading Regge singularity near $J=1$ in the complex angular momentum plane, the Pomeron,[1] it has been recognized that among all Regge singularities the Pomeron is unique in many ways. Experimentally, it is not clearly associated with resonances, as are the ρ and f trajectories, for example, and its slope at $t=0$ appears to be half or less than half of the slopes of other trajectories.[2] And theoretically, in one of the most successful models of Regge behavior to date, namely the dual resonance model, it is not present in the Born or the tree approximation, but arises through unitarity as an entirely new singularity.[3] In 1968 Chew and Pignotti proposed a multiperipheral model of the Pomeron which regarded it in the first approximation as a factorizable Regge pole with an intercept close to $J=1$.[4] They suggested, furthermore, that it should couple weakly in hadronic processes. Thus cross sections involving double-Pomeron exchange, for example the process $pp \to pfp$ at high energies with the f meson nearly at rest in the c.m. system, were predicted to be quite small compared to elastic cross sections, which would involve only single-Pomeron exchange. This is found to be correct experimentally.[5]

In keeping with the assumed weakness of the Pomeron-pole coupling Chew and Pignotti obtained the pole contribution to the total cross section by summing inelastic cross sections in which no Pomeron exchanges were included. When they allowed the Pomeron pole to be exchanged once as in elastic scattering, they obtained the two-Pomeron-cut contribution to the total cross section as a next-order correction to the description of the Pomeron singularity.

The Chew-Pignotti model was successful in accounting for a number of experimental results. The basic features of short-range order in the multiperipheral model were connected theoretically to the factorization of the Pomeron pole.[6] Factorization seems to be reasonably well satisfied (within experimental errors of 30%) by measured quasielastic differential cross sections[7] and inclusive reactions.[8] And short-range order would account indirectly for the approximate Poisson distribution of the measured multiplicity of secondaries, the $\ln s$ growth of the average multiplicity, the approximate plateau in the single-particle inclusive cross section as a function of rapidity, and, most directly, for the decorrelation of secondaries at increasing rapidity separation observed in two-particle inclusive reactions at the CERN ISR.[9]

The idea of treating the coupling of the Pomeron as a small parameter later received considerable attention through the development of the multiperipheral version of the two-component model of multiple production,[10] the first component being associated with production amplitudes free of Pomeron exchanges, i.e., with small rapidity gaps which sum up to produce a Pomeron pole in the total cross section, and the second being associated with single-Pomeron exchanges, i.e., one large rapidity gap in the production amplitudes and a two-Pomeron cut in the total cross section. The multiperipheral version permitted a natural generalization to a third component, etc., through the introduction of extra Pomeron exchanges in the production amplitudes, though the contribution of these components was thought to be quite small at energies in the few-hundred-GeV range.

Both the Chew-Pignotti and two-component models, however, suffered from the neglect of unitarity in the t channel. Gribov, Pomeranchuk, and Ter-Martirosyan, and more recently White, have shown, starting with four-body unitarity, that it is possible to derive rigorous formulas for the discontinuity of J-plane cuts arising from two fac-

torizable Regge poles.[11] They also suggested a plausible generalization to cuts involving three or more Regge poles. As a consequence of these "J-plane unitarity" formulas they were able to determine the sign of the two-Pomeron cut quite rigorously in terms of its signature. Their result was that the two-Pomeron cut should contribute negatively to the total cross section in contrast to the positive result of the multiperipheral model. The discrepancy, as many have since observed, could be traced to the fact that the first component of the two-component model, i.e., the small-rapidity-gap component has a high-energy behavior typical both of a pole and a cut, the latter being smaller and contributing negatively to the cross section, so as to reverse the sign of the contribution of the second component.[12]

The multiperipheral model had not attempted to incorporate t-channel unitarity at the level of the four-body intermediate state, and so it was not surprising that it was found to be in conflict. The crucial observation of Gribov, Pomeranchuk, and Ter-Martirosyan was that such a consideration was indeed very relevant to the description of the two-Pomeron-cut singularity.

Gribov in subsequent work proceeded to study the properties of the J-plane discontinuity formulas and constructed a model solution to the discontinuity equations based on a $\lambda\phi^3$ perturbation theory in which the Pomeron pole was taken to be the leading pole in off-shell 2-2 scattering amplitudes in the graphs.[13] The perturbation-theory solution was also extremely useful for obtaining discontinuity formulas for more complicated J-plane cuts,[14] since the rigorous derivation from multibody t-channel unitarity is extremely laborious. Gribov considered only a particular class of perturbation graphs, but his treatment was sufficiently general to provide a basis for the formulation of the Reggeon calculus, i.e., a set of rules somewhat analogous to the Feynman rules in operator field theory for constructing a perturbative expression for the t-channel partial-wave amplitudes which satisfies the J-plane discontinuity equations. Gribov and Migdal[15] then exploited further the analogy between the J-plane discontinuity formulas and ordinary nonrelativistic energy-plane unitarity to show that the calculus was equivalent to the perturbative solution of a nonrelativistic field theory in two dimensions in which the Pomerons appeared as scalar fields.

Subsequent research concentrated on investigating solutions of the formal Reggeon field theory.[15] Because of the complexity of the problem, it was necessary to make various approximations, including neglecting all trajectories but the Pomeron, replacing the Pomeron form factors by constants, ignoring terms to order $(\ln s)^{-1}$, and requiring that the renormalized Pomeron be strictly factorizable with an intercept of precisely $J=1$. Some approximate solutions were obtained. Their relevance to the real world was always subject to some doubt, since it was not possible to know *a priori* which model Lagrangian represented a "correct" theory of the Pomeron. Because of the approximations used it was never clear, when experiment disagreed with theory, whether the approximations were at fault or the model Lagrangian was incorrect. There was a concerted effort to determine the precise nature of the Pomeron singularity, which in turn would control the ultimate asymptotic behavior of scattering amplitudes. However, one could not determine whether present accelerators provided suitably asymptotic energies.

Within the past year renormalization-group techniques have been successfully applied to the Reggeon field theory.[16] It is now possible to determine the precise nature of the Pomeron singularity and its associated cuts within the confines of restricted choices for the Lagrangian in the Reggeon field theory. The drawbacks of focusing on a precise description of the Pomeron and neglecting the rest of the J plane are the same as before—one is reconciled to an extremely asymptotic representation of scattering amplitudes. Also the flexibility in the choice of Lagrangians leads to a lack of definiteness in the solution. It is hoped that future work on this powerful approach will be able to treat more realistic Lagrangians with more physical Pomeron form factors and with other trajectories. However, as we discuss below, there may be serious drawbacks to a total devotion to the J plane.

It is possible that, in order to understand the Pomeron sufficiently well to explain experimental results, it is necessary to find a solution to the Reggeon field theory as in the renormalization-group approach. We would like to explore an alternative and highly appealing possibility that one may be able to exploit the weakness of the Pomeron coupling and therefore use low-order perturbation theory as a basis for an understanding of phenomenology. In other words, it would be extremely practical to wed the phenomenological simplicity of the two-component model[10] with the theoretical insight of the Reggeon calculus.[17]

A number of others have also advocated this approach to understanding the Pomeron, especially Ter-Martirosyan.[18] The key feature which we want to stress is a description of scattering processes at accessible energies. This precludes making an expansion in powers of $(\ln s)^{-1}$, which has been the traditional practice in the Reggeon

calculus. Rather, we would advocate an expansion in $g\ln s$ where g characterizes the small Pomeron coupling and $\ln s$ is not too large. Moreover, we would advocate relaxing the requirements that in phenomenological applications, the Pomeron intercept be taken to be exactly $J=1$ and that the triple-Pomeron coupling vanish, a practice which had been motivated by a special solution to the formal field-theoretic version of the Reggeon calculus.[15] And finally we would like to free the calculus as nearly as possible from any reference to a specific underlying field theory (such as $\lambda\phi^3$) and isolate its essential S-matrix features.

For a practical phenomenology, there are a number of good reasons for adopting a perturbative approach rather than seeking exact solutions to the Reggeon field theory. It may happen, for example, that the intermediate-energy behavior of amplitudes differs markedly from the ultimate high-energy behavior. For example, suppose that the true J-plane structure of the Pomeron had the form suggested by some multiperipheral models[19]

$$A(J)=\frac{\beta_a\beta_b}{J-\alpha_0+g^2\ln(J-1)}$$
$$=\frac{\beta_a\beta_b}{J-\alpha_0}\left[1-\frac{g^2\ln(J-1)}{J-\alpha_0}+O(g^4)\right], \qquad (1.1)$$

where $\mathrm{Re}\alpha_0<1$ and $\mathrm{Im}\alpha_0=0$. This amplitude is exactly described by a cut extending up to $J=1$ and a pair of poles where the denominator vanishes. If g^2 is small, these poles are at

$$J\approx\alpha_0-g^2\ln(1-\alpha_0)\pm i\pi g^2 .$$

As long as α_0 is near 1 and $g^2\ln(1-\alpha_0)$ is small, the low-energy behavior of the total cross section is approximately given by

$$\sigma(s)\propto\beta_a\beta_b s^{\alpha_0-1}[1+O(g^2\ln s)+O((1-\alpha_0)\ln s)], \qquad (1.2)$$

as may be seen by the expansion in Eq. (1.1). This behavior is more characteristic of the pole than of the cut. At very high energies, the cut dominates the asymptotic behavior and one finds

$$\sigma(s)\sim\frac{\beta_a\beta_b}{g^2\ln s\,(\ln\ln s)^2}, \qquad (1.3)$$

which is quite different from the lower-energy behavior. Thus a study of the precise nature of the branch-point singularity could conceivably be of little relevance to present-day experiment if the cut were sufficiently weak.

As another example, suppose the high-energy behavior of the cross section is described by a function of the form

$$\sigma(s)\sim\beta_a\beta_b\left(s^\epsilon-\frac{\beta^2s^{2\epsilon}}{2!}+\frac{\beta^4s^{3\epsilon}}{3!}-\cdots\right)$$
$$=\frac{\beta_a\beta_b}{\beta^2}[1-\exp(-\beta^2s^\epsilon)], \qquad (1.4)$$

an expression somewhat reminiscent of the Cheng and Wu model of the Pomeron.[20] If ϵ were positive, then at energies sufficiently low, i.e., such that $\beta^2s^\epsilon\ll1$, the cross section would be dominated by the first term

$$\sigma(s)\sim\beta_a\beta_b s^\epsilon[1+O(\epsilon\ln s)], \qquad (1.5)$$

corresponding approximately to a factorizable pole at $J=1+\epsilon$, whereas at very high energies the behavior would be quite different,

$$\sigma(s)\sim\frac{\beta_a\beta_b}{\beta^2}, \qquad (1.6)$$

corresponding to the true singularity at $J=1$. Once again, knowing the properties of the actual singularity at $J=1$ would be of little practical relevance to the intermediate-energy behavior.[21] Moreover, we see in this example that a description based solely on the J plane is entirely inadequate. The first series corresponds to a sequence of poles advancing toward $J=+\infty$:

$$A(J)\propto\beta_a\beta_b\left(\frac{1}{J-1-\epsilon}-\frac{\beta^2}{2!}\frac{1}{J-1-2\epsilon}\right.$$
$$\left.+\frac{\beta^4}{3!}\frac{1}{J-1-3\epsilon}-\cdots\right), \qquad (1.7)$$

which is convergent for any J and clearly does not sum to the J-plane representation of (1.6) when $\epsilon>0$, namely,

$$A(J)\propto\frac{\beta_a\beta_b}{\beta^2(J-1)}. \qquad (1.8)$$

In other words, the Froissart-Gribov partial-wave projection cannot always be interchanged arbitrarily with a perturbation-series expansion. However, the correspondence between (1.4) and (1.7) is correct for a finite number of terms. In the Reggeon calculus a bare-Pomeron pole at $J=1+\epsilon$ corresponds to a tachyon field which is pathological and requires unusual means to incorporate into a consistent theory.[22] Nevertheless, if one is content with obtaining only the first few terms in the series expansion, without dealing with the problem of actually solving the theory with a negative mass, the terms can be accurately reproduced by the Reggeon calculus.

As we have seen in these examples, keeping in close touch with the energy behavior of various terms in the series expansion of a scattering amplitude makes it possible to formulate an approximation to the scattering amplitude which is based on the smallness of an energy-dependent parameter of the form $\epsilon\ln s$ or $g^2\ln s$. At high energies the approximation cannot be made. Specifying the amplitude over a limited range of energies corresponds to an imprecise specification of the J-

plane properties, a concept which is difficult to define in J-plane language as the second example shows.

Another complication which arises in expressing high-energy behavior in the J-plane language, which is more readily treated in a perturbative approach in terms of energy behavior, is the threshold phenomenon. Suppose we were to extend the two-component model to describe multiple production at very high energies in terms of the diffractive production of several "fireballs" (Fig. 1) (i.e., with multiple Pomeron exchange). If there were a minimum fireball mass, there would be an upper bound to the number of fireballs that could be produced at any finite energy. At increasing energies, more fireballs could be produced. This phenomenon was studied by Chew and Snider and others in the context of the multiperipheral model.[23] They found that the total cross section would undergo a mild damped oscillation about an average power-law behavior, rising above average at the thresholds of multifireball production and falling below average in between. They found that such an effect corresponded in the J plane to a pair of complex poles in addition to the predominant leading singularity usually associated with the Pomeron. It is difficult enough to cope with a single pole singularity in present efforts to find exact solutions to the Reggeon field theory, let alone introduce new complex poles. However, a perturbative approach could deal with the energy dependence of the individual multifireball cross sections one by one, thereby avoiding the necessity of introducing complex poles.

For these reasons we believe that it is at best inconclusive and at worst possibly erroneous to base a theory of high-energy scattering on J-plane considerations alone. However, it may be reasonable for phenomenological applications to use the insights into J-plane structure which the Reggeon calculus has provided in order to treat Reggeon couplings in a perturbative way in parallel with an energy-plane description of the scattering amplitudes. In an effort to make the contact between J-plane and energy-plane descriptions more secure, we have reviewed the foundations of the Reggeon calculus in perturbation theory in Sec. II.

There is at present no direct derivation of the Reggeon calculus based solely on the axioms of S-matrix theory, although the guiding principle, namely the existence of J-plane discontinuity equations, has been shown to follow from t-channel unitarity. The most direct axiomatic derivation would have to proceed along the same route as in the rigorous proof of the J-plane discontinuity equations,[11] starting from t-channel unitarity, defining the Froissart-Gribov continuations of J-plane amplitudes in several angular momentum variables and making the appropriate continuations to the negative t region, while at the same time isolating from the full amplitudes those parts containing singularities of the Pomeron. This method is arduous and pedagogically awkward and so we have chosen, instead, to follow in Gribov's footsteps and seek a derivation of the Reggeon calculus based on $\lambda\phi^3$ perturbation theory with some general assumptions about the Regge singularities. We believe that most of the assumptions we make must also appear in some form in an axiomatic approach. Thus even though we rely on perturbation theory as a guide, the results should be the same as though they had been derived from first principles alone. Another advantage of starting with perturbation theory is that this ensures that the resulting theory of the Pomeron is a perturbative expression of t-channel as well as s-channel unitarity.

The basic ingredients of the Reggeon calculus are a bare singularity, which we call a bare Pomeron (even though we call it a Pomeron, we shall keep the discussion general enough that other types of trajectories may be substituted) to distinguish it from the physical Pomeron in the full amplitudes, and bare amplitudes for the scattering of Pomerons and/or particles. The bare or lowest-order N-point amplitudes in the Pomeron perturbation series are taken to be fully consistent with S-matrix principles in all respects except that they contain no Pomeron-pole singularities, branch points, or other singularities which result from the iteration of the Pomeron pole. For the moment no assumptions are made about the dynamical origin of the bare singularity or of its nature, except that it must be a factorizable pole. Later on it may be useful to associate the absorptive part of the bare Pomeron with the short-range correlation component of the two-component model.

It is traditional in S-matrix theory to imagine that it is possible to construct an S matrix free of electromagnetic interactions, yet otherwise consistent with the basic axioms. Usually, the electromagnetic interactions are subsequently introduced using perturbation theory. The bare amplitudes are those involving N particles and M external photons, but no internal photons. The success of such an approach rests on the smallness of the photon coupling constant. The Reggeon calculus provides a mechanism for treating the Pomeron in a similar way. Because of the composite nature of the Pomeron, it is necessary to resort to more sophisticated techniques. Of course, the Pomeron coupling is probably not as weak as that of the photon.

A precise definition of a bare Pomeron in terms

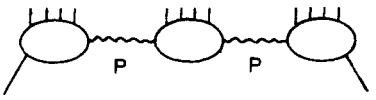

FIG. 1. Diagram for "multifireball" production.

of the physical amplitudes is not possible without specifying how amplitudes involving cuts are to be separated from those involving only poles. This will become apparent below. This same problem arises in the multiperipheral version of the two-component model. There it is convenient to classify multiple production events on the basis of the number of large rapidity gaps. If there are no gaps Δy larger than L, then the event is classified as a nondiffractive event (first component). If there is only one gap $\Delta y > L$ then the event is classified as diffractive (second component). In the latter case one parameterizes the production amplitude with a single bare-Pomeron exchange and this leads to a bare-two-Pomeron-cut behavior of the total cross section. The bare-Pomeron-pole behavior is obtained from the first component. Obviously, changing the value of L changes the separation between the two components and therefore the definition of the bare Pomeron. The sum of all components (first, second, third, etc.) is of course invariant with respect to the value of L. In the language of renormalization, redefining L amounts to a partial renormalization of the bare Pomeron. In the limit $L \to \infty$ the "bare Pomeron" must be the same as the fully renormalized Pomeron. In principle, the calculation must be independent of L. In practice, however, L must be chosen on the one hand to be large enough that exchanges other than the Pomeron can be ignored and the convergence of the perturbation series is rapid owing to the small amount of renormalization, yet on the other hand to be small enough that it is not necessary to choose a bare Pomeron which looks just like the actual Pomeron, and contact with experiment at least at the level of the second component becomes possible.

The necessity of introducing a cutoff dependence in the perturbation expansion and the related indefiniteness of the choice of the bare-Pomeron intercept is one of the chief drawbacks to the perturbative approach. Moreover, in the context of a perturbation theory with an only approximate treatment of unitarity in both t- and s-channels the old decoupling questions,[24] which pertain to physical and not bare Pomerons, cannot be resolved. Indeed the bare-Pomeron intercept is permitted to lie above $J=1$ as freely as below. And of course, by using perturbation theory, one is retreating from confronting the larger question of what the Pomeron really is. But the relative simplicity and potential practicality of the perturbative approach make it well worth some study.

The formal procedure for obtaining the calculus from $\lambda\phi^3$ perturbation theory is discussed in concrete terms in Sec. II. The organization of the remainder of the paper is as follows. In Sec. III we rederive expressions in the Reggeon calculus for diagrams contributing to the two-Pomeron cut. In addition to incorporating the cutoff dependence required in Sec. II we also make use of the current understanding of the treatment of signature in multi-Regge amplitudes.[25] The results agree basically with those of Gribov but differ in some details. The discrepancies are noted in Sec. IV, and in Sec. V. we collect some formulas useful for phenomenological application.

II. REVIEW OF THE FOUNDATIONS OF THE REGGEON CALCULUS IN PERTURBATION THEORY

Gribov and collaborators first obtained the Reggeon calculus using $\lambda\phi^3$ perturbation theory. They chose a restricted set of graphs, but clearly intended that their results should follow equally well from a more general set of graphs. We would like to adopt the more general approach so as to draw attention to the essential assumptions.

To begin with, it is necessary to have a model for the Pomeron pole so that it can be clearly identified in a topological way. It is convenient, but not necessary, to choose the usual ladder without crosses as a starting point. The sum of the ladder graphs (Fig. 2) is well known to produce Regge-pole singularities.[26] We shall take the leading Regge pole of the ladder as an initial definition of the bare Pomeron, with the reservation that it is subject to renormalization yet to be specified before obtaining the final bare Pomeron. It is understood, of course, that the ladders in Fig. 2 are evaluated taking Bose symmetry into account so as to produce the positive-signatured trajectory.

The goal is to classify all graphs in $\lambda\phi^3$ perturbation theory for the four-particle amplitude for the process $ab \to a'b'$ in terms of their contribution to the diagrams of Fig. 3. These diagrams are characterized by *basic 2n-point scattering amplitudes*, which are connected in the sense that there is no cluster decomposition that separates them so as to make one of the higher order diagrams, and a *two-body propagator* denoted by the box labeled P constructed from the renormalized ladders, and they are summed in such a way that,

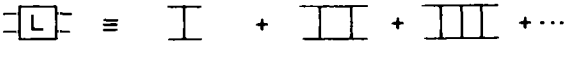

FIG. 2. Ladder graphs.

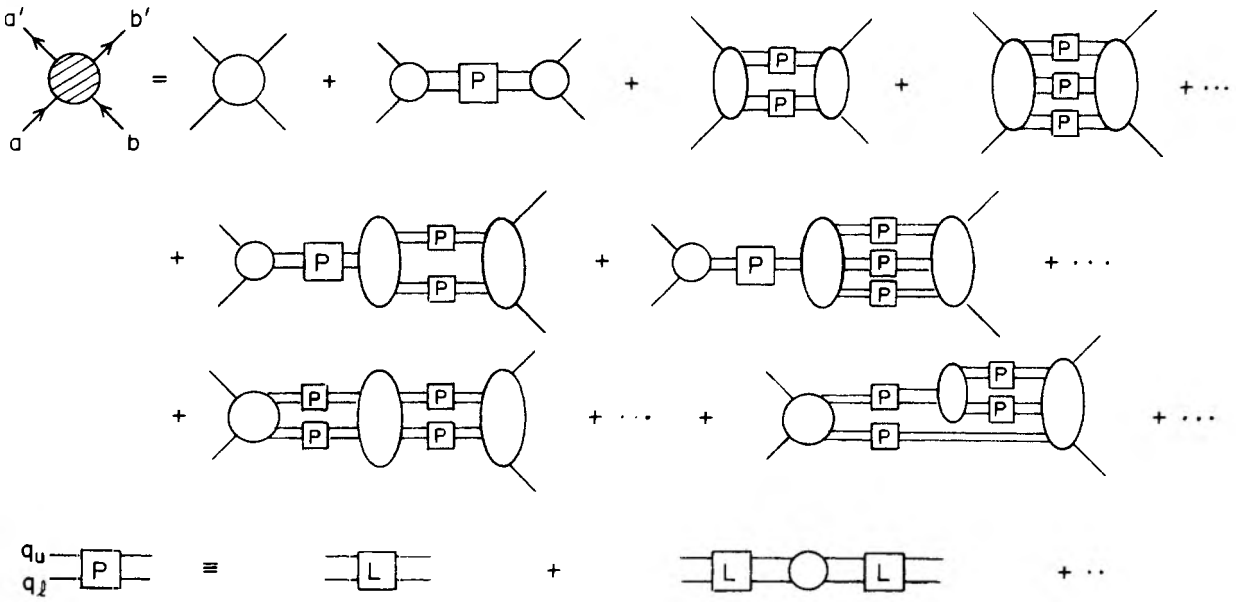

FIG. 3. Decomposition of 2-to-2 amplitude and definition of "two-body propagator."

reading from left to right, the propagators alternate with the basic amplitudes, with all possible numbers of propagators at each position and all possible couplings of propagators to the basic $2n$-point amplitudes at each position. The propagators are eventually to be identified with the bare Pomeron and the basic amplitudes with Pomeron-free scattering amplitudes.

We must formulate a procedure for associating a general graph in $\lambda\phi^3$ perturbation theory with one or more of the diagrams of Fig. 3 in a systematic way so that all graphs may be included, but no graph is included twice. In other words, it is necessary to define the basic $2n$-point amplitudes so that they cannot be further decomposed in terms of the two-body propagators. This is accomplished by dividing up the loop integrations so that in each diagram various cutoff criteria are satisfied.

First we require that the four-momentum of the two-body propagators as indicated in Fig. 3

$$q = q_l + q_u , \tag{2.1}$$

be cut off in the loop momentum integration so that

$$|q^2| \lesssim T \approx O(1) , \tag{2.2}$$

where we use units of 1 GeV for the masses.

We also want to arrange so that the subenergies across the two-body propagators are sufficiently high that they may be replaced by the Pomeron. To do this, it is useful to distinguish between the case in which a two-body propagator appears alone and in which it appears together with others. In the former case (see Fig. 4) all possible "subenergies" constructed from the four-momenta of the adjacent two-body propagators or external particles must be larger than a large squared mass Δ,

$$|s_{ij}| = |(q_i - q_j)^2| \gtrsim \Delta , \tag{2.3}$$

where q_i is chosen from the set on the left and q_j from the set on the right. In the latter case we consider all possible ways of grouping the two-body propagators coupling into the two adjacent basic scattering amplitudes both incoming and outgoing so that a "cluster mass" is defined. A cluster mass is the invariant mass exchanged between two-body propagators. For example, two of the cluster masses of Fig. 5 are the invariants corresponding to the four-momenta crossing the dotted lines, i.e.,

$$\begin{aligned} M_{13}^{\ 2} &= (q_1 - q_3)^2 , \\ M_{36}^{\ 2} &= (q_3 - q_6)^2 . \end{aligned} \tag{2.4}$$

We then require that the over-all subenergy must substantially exceed the cluster masses, e.g., if

$$s_{16} = (q_1 - q_6)^2 \tag{2.5}$$

then

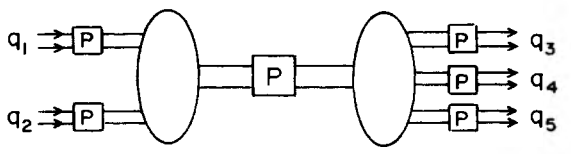

FIG. 4. Section of diagram involving one two-body propagator.

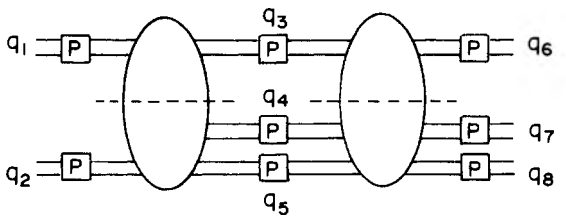

FIG. 5. Section of diagram involving more than one two-body propagator.

$$\delta |s_{16}| \gtrsim |M_{13}{}^2| \, |M_{36}{}^2|, \tag{2.6}$$

where δ is a very small squared mass. This must be true for all possible definitions of the cluster masses. (If the propagator on the right or left in Fig. 5 consists of a single two-body propagator, then it is necessary to include the next basic amplitude when defining the cluster masses.)

The basic $2n$-point scattering amplitudes are defined so that they cannot be further decomposed in terms of ladders (as defined in Figs. 2 and 3) and subject to the above constraints on the integrations over loop momenta. Thus the correspondence between a given graph in $\lambda\phi^3$ perturbation theory and the diagrams of Fig. 3 may be found by examining its integration over loop momenta according to the various schemes of Fig. 3. In general it will be found that the given graph contributes to several of the diagrams of Fig. 3, corresponding to the full range of integration over the various loop momenta. For example, the graph of Fig. 6 contributes to the two diagrams shown. (The ovals in this figure were drawn to help in visualizing the basic $2n$-point scattering amplitudes, which must be connected in the sense that no ladders pass completely through without at least one of the pairs of particles interacting. The ladders are all of minimum length.) The example of Fig. 6 is also amusing since it shows that the decomposition into diagrams of Fig. 3 cannot be based on the apparent topology alone. One might think it would be easy to look at a graph and see the ladders. However, as the example shows, sometimes it depends on how one looks at one graph whether it conforms to one topology or another. In fact, we *do* want to count the graph in different ways depending on the values of the integration variables, and so it is necessary to introduce a cutoff to avoid multiple counting.

With these observations in mind it seems quite reasonable to expect that one can systematically assign a given graph in perturbation theory to a set of diagrams of Fig. 3. Suppose one starts by finding a highly complicated (high-order) diagram in Fig. 3 that conforms topologically to the graph in perturbation theory, to the extent that the two-body propagators contain ladders of at least the minimum number of rungs and the bubbles are connected. Over some part of the range of integration over loop momenta, the cutoff criterion for the diagram of Fig. 3 must be satisfied. Related to this most complicated diagram is a family of simpler diagrams obtained by contracting adjacent bubbles in all possible ways. The family always contains the first and simplest diagram in Fig. 3. When the cutoff criterion for one diagram fails to be satisfied, there is always a simpler diagram in the family which takes over.

Within a particular family of diagrams related in this way to a single most complicated diagram, there is no question that the perturbation-theory graph is made to contribute once and only once to each diagram, since one progresses to more complicated graphs in this family by dividing the bubbles in such a way that the newly formed bubbles are joined by one or more two-body propagators—as soon as this operation can be performed in keeping with the cutoff criterion the contribution from the perturbation-theory graph must shift. However, if one imagines progressing in this way from simpler graphs to more complicated graphs, one might be concerned that there may in general be several distinct terminal branches of the "family tree" corresponding to the most complicated (highest-order) diagram of Fig. 3 in a given sequence. In other words, there may in general be different ways of dividing bubbles, which lead ultimately to two different diagrams which cannot be made more complicated. However, although no rigorous proof is given here, it seems rather likely that for every graph there is a unique diagram, which is the most complicated. It is characterized by the simplest connected bubbles, i.e., ones which cannot be further divided. Should this be the case, then the contributions are uniquely assigned.

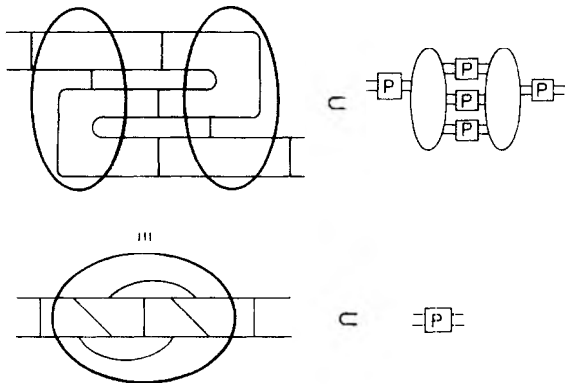

FIG. 6. Example of correspondence between graphs and diagrams.

An alternative to the cutoff procedure is to specify an arbitrary low-subenergy extrapolation of the Pomeron-pole behavior in the two-body propagators. The difference between this extrapolation and the two-body propagator has itself no Pomeron pole and so can be assimilated into a lower-order diagram. This procedure is also arbitrary in its choice of the low-subenergy extrapolation, and so we prefer to use the more vivid, arbitrary cutoff technique.

We now make the key assumption which permits the formal construction of the Reggeon calculus, namely that the leading Regge singularity in the two-body propagator is a factorizable pole which we call the bare Pomeron, and the basic $2n$-point amplitudes do not contain this pole (or cuts derived from it). This is plausible if the pole in the ladder sum is not greatly altered by the partial renormalization which takes place in constructing the two-body propagator in Fig. 3. If the pole owes it existence primarily to the ladder sum, then one does not expect it to appear in the basic $2n$-point amplitudes, since they do not contain ladders of arbitrarily high mass. However, if the pole owed its existence instead to a three-body channel, for example, and was only slightly renormalized by two-body coupling, it could then appear at a slightly shifted position in the basic $2n$-point amplitudes and the formalism would be useless as it stands. In the latter case, however, rephrasing the decomposition in terms of the three-body channel would provide an acceptable alternative.

The final step in the construction of the Reggeon calculus is to replace the two-body propagator by the leading Regge-pole contribution, namely a product of factorized pole residue and propagator as illustrated in Fig. 7 and then to complete the loop integration on the residues, thereby constructing the bare-Pomeron scattering amplitudes. The result is illustrated in Fig. 8. This step may be justified in the following way. We shall ultimately find that in the limit $s \to \infty$ the integrations over loop momenta reduce to integrals over discontinuities of the basic scattering amplitudes as a function of their cluster masses. These discontinuities are in turn associated with a particular on-mass-shell intermediate state. The high-subenergy cutoff (2.6) then corresponds precisely to the same momentum space separation of the particles of the two adjacent clusters that is traditionally assumed in order to justify a Regge-pole approximation.

FIG. 7. Example of notation for the bare-Pomeron trajectory and scattering amplitude.

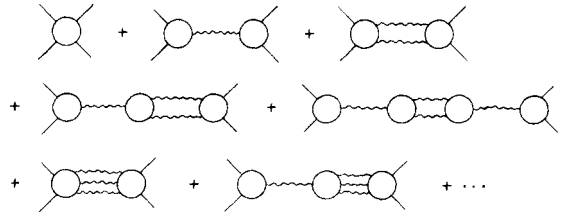

FIG. 8. Reggeon diagrams after inserting bare Pomerons.

In characterizing the diagrams of Fig. 3 we required that the subenergies be cut off at a value much larger than the cluster masses. Changing the cutoff leads to a redefinition of the basic $2n$-point amplitudes. As mentioned earlier, this also leads to a partial renormalization of the bare Pomeron. For example, increasing the cutoff would subtract from the first diagram of Fig. 6 and add to the second. The two effects compensate each other so that the sum of the diagrams is unaltered. However, the choice of the cutoff is not entirely arbitrary. For the purposes of introducing the Pomeron contribution it must be large.

For subsequent discussion it is convenient to define new bare amplitudes which add in the bare-Pomeron poles but no cuts. Thus we rewrite the diagrams of Fig. 8 as shown in Fig. 9, where the shaded bubble denotes the presence of Pomeron poles.

Now we are not really interested in $\lambda\phi^3$ perturbation theory, save as a paradigm; and so it is desirable to seek a generalization. Evidently, it should be possible to exploit the factorizability of the Pomeron to construct the diagrams of Fig. 8 from a set of basic scattering amplitudes involving Pomerons and particles connected with a Pomeron propagator. Through factorization, it should be possible to obtain the Pomeron scattering amplitudes from the appropriate asymptotic limit of the basic $2n$-point functions as illustrated in Fig. 10.

The problem is then to find a set of rules for constructing the diagrams of Fig. 8 consistent with the factorization property and what has been learned from $\lambda\phi^3$ perturbation theory but without specific reference to the details of $\lambda\phi^3$ theory. It is also useful to discuss the asymptotic behavior of these diagrams as $s \to \infty$ with t fixed by carrying out a Mellin transform in the variable s. (We

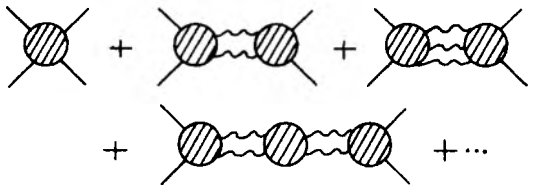

FIG. 9. Diagrams in terms of amplitudes containing Pomeron poles.

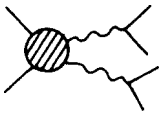

FIG. 10. Six-point function containing bare-Pomeron–particle amplitude.

use the Mellin transform in place of the Froissart-Gribov continuation as a matter of convenience.) The Mellin representation of the diagrams of Fig. 8 is the foundation of Gribov's Reggeon calculus. This general construction is discussed in the following sections.

III. A CONSTRUCTION OF THE REGGEON CALCULUS

A. The Reggeon-particle-cut diagram

1. Singularities of the integrand

To illustrate the techniques we shall use in obtaining the Mellin transforms of the diagrams of Fig. 9 we consider the simple diagram of Fig. 11. (This diagram is not included in the set of diagrams in Fig. 9, since we are concerned here with theories in which all particles lie on Regge trajectories. However, it is pedagogically useful.) The exchange in this case consists of a Reggeon and a scalar particle which may generate a fixed J-plane cut. In this simple example, the singularity structure of the integrand in this graph can be obtained

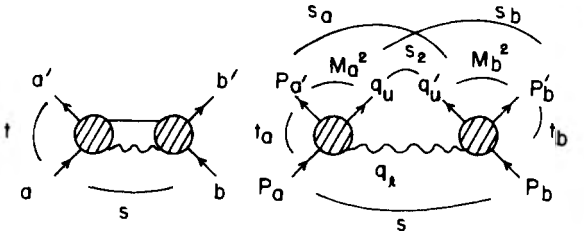

FIG. 11. Diagram with J-plane cut. Notation for integration.

directly from the six-particle amplitude also shown in Fig. 11. Let us define the channel invariants in terms of the momenta indicated in Fig. 11.

$$\begin{aligned} &M_a^2=(p_a-q_1)^2,\quad u_a=(p_{a'}+q_1)^2,\\ &M_b^2=(p_{b'}+q_1)^2,\quad u_b=(p_{b'}-q_1)^2,\\ &s=(p_a+p_b)^2,\quad s_a=(p_{a'}+q_u+q_u')^2,\\ &t_1=q_1^2,\quad s_b=(p_{b'}+q_u+q_u')^2,\\ &t_u=q_u^2,\quad s_2=(q_u+q_u')^2,\\ &t_u'=(q_u')^2,\quad t_a=q^2,\quad q=p_a-p_{a'},\\ &t_b=(p_{b'}-p_b)^2. \end{aligned} \tag{3.1}$$

If the six-particle amplitude is written as a function of the channel invariants

$$T_6(M_a^2,M_b^2,s,t_a,t_b,t_1,s_a,s_b,s_2;t_u,t_u'), \tag{3.2}$$

then the contribution to the four-point amplitude of Fig. 11 is

$$\bar{A}_1(s,t)=\frac{-i}{(2\pi)^4}\int_D d^4q_1\,\frac{1}{t_u-m^2}\,T_6(M_a^2,M_b^2,s,t_a=t,t_b=t,t_1,s_a=m^2,s_b=m^2,s_2=0;t_u,t_u'=t_u), \tag{3.3}$$

where the domain D of the integration is specified by the cutoff prescription of the previous section, namely

$$\begin{aligned} &|t_1|,\ |t_u|\lesssim O(1),\\ &\delta|s|\gtrsim|M_a^2|\ |M_b^2|. \end{aligned} \tag{3.4}$$

The factor $-i/(2\pi)^4$ gives a positive imaginary part to the scalar box graph above threshold in s.

In order to evaluate the asymptotic limit of $\bar{A}_1(s,t)$ at large s, fixed t, it is necessary to know the singularity structure and asymptotic behavior of the integrand itself. We assume it is permissible to interchange the asymptotic limit with the cutoff integration. Therefore, we must consider an asymptotic limit of the amplitude T_6 as $s\to\infty$ with all other variables listed in (3.1) fixed. This is called the helicity asymptotic limit and the properties of the six-particle amplitude in this asymptotic regime have been deduced from some rather general assumptions about the singularity structure and Regge behavior.[25]

As an illustration of the required asymptotic behavior, let us suppose for the moment that the amplitude T_6 has a simple pole in M_b^2 so that

$$T_6=T_5(M_a^2,s_b,s,t_a,t_1)\,\frac{1}{M_b^2-m^2}, \tag{3.5}$$

corresponding to the diagram of Fig. 12. In this case the helicity asymptotic behavior of T_6 is determined by T_5, namely[25]

$$\begin{aligned} T_5 \underset{s\to\infty}{\sim}\ &\bar{B}_a(M_a^2,t_a,t_1)\,\Gamma(-\alpha_1)\tfrac{1}{2}[(-s)^{\alpha_1}+\tau_1 s^{\alpha_1}]\,\beta_b(t_1)\\ &+f(s_b,t_a,t_1)\tfrac{1}{2}[(-s)^{\alpha_a}+\tau_a s^{\alpha_a}], \end{aligned} \tag{3.6}$$

where $\alpha_1=\alpha_1(t_1)$ and $\alpha_a=\alpha_a(t_a)$ are the leading

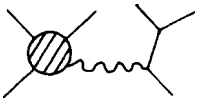

FIG. 12. Simplified six-particle amplitude.

Regge trajectories in the t_a and t_l channels and τ_l and τ_a are the corresponding signatures. The trajectory α_l is the bare-Pomeron trajectory and the factorization of its residue is shown explicitly in (3.6). The first term of (3.6) is characteristic of the Pomeron and also contains right- and left-hand cuts in M_a^2. The second term is entire in M_a^2, depends on trajectories in the t_a channel, and does not factor in the same way as the first. The second term has not been considered in the conventional derivation of the Reggeon calculus,[13] although it turns out that it does not contribute to the J-plane projection because it has no associated discontinuities in M_a^2. (See Appendix A.) The information about t_a-channel Regge poles, contained in the second term, is duplicated in the first, since the high M_a^2 behavior depends on α_a in the following way:

$$T_5 \underset{\substack{s\to\infty \\ M_a^2\to\infty}}{\sim} \beta_a(t_a)\,\Gamma(-\alpha_a+\alpha_l)\tfrac{1}{2}[(-M_a^2)^{\alpha_a-\alpha_l}+\tau_a\,\tau_l(M_a^2)^{\alpha_a-\alpha_l}]\,\gamma(t_a,t_l)\,\Gamma(-\alpha_l)\tfrac{1}{2}[(-s)^{\alpha_l}+\tau_l s^{\alpha_l}]\,\beta_b(t_b)$$
$$+(\text{term entire in } M_a^2)\ . \tag{3.7}$$

The same analysis applied to the general six-particle amplitude yields an expression similar to (3.6):

$$T_6 \underset{s\to\infty}{\sim} \bar{B}_a(M_a^2,t_a,t_l,t_u)\,\Gamma(-\alpha_l)\tfrac{1}{2}[(-s)^{\alpha_l}+\tau_l s^{\alpha_l}]\,\bar{B}_b(M_b^2,t_b,t_l,t_u')+(\text{other terms}), \tag{3.8}$$

where the other terms are entire in either M_a^2 or M_b^2 or both. In anticipation of the result that only terms with discontinuities in M_a^2 and M_b^2 contribute to the J-plane projection, we drop the other terms from our formulas.

2. *Evaluation of the Mellin transform*

We return to the integral (3.3) with the replacement (3.8), which is assumed to be valid in the domain D:

$$\bar{A}_1(s,t)\simeq\frac{-i}{(2\pi)^4}\int_D d^4q_l\,\bar{B}_a(M_a^2,t,t_u,t_l)\frac{\Gamma(-\alpha_l)}{t_u-m^2}\tfrac{1}{2}[(-s)^{\alpha_l}+\tau_l s^{\alpha_l}]\,\bar{B}_b(M_b^2,t,t_u,t_l)\ . \tag{3.9}$$

A detailed analysis of this integral is given in Appendix B, but for an approximate and less cluttered approach, it is convenient to use the Sudakov variables.[27] The approximations have the effect of neglecting a kinematic cutoff in D, but these can be easily incorporated at the end. As usual, we define the basis vectors

$$p_\alpha=p_a-\frac{m^2}{s}p_b\ ,\quad p_\beta=p_b-\frac{m^2}{s}p_a\ , \tag{3.10}$$

so that

$$p_\alpha^2=O(1/s),\quad p_\beta^2=O(1/s),\quad p_\alpha\cdot p_\beta=s/2\ , \tag{3.11}$$

and any vector, in particular q_l, may be written

$$q_l=\alpha p_\alpha-\beta p_\beta+Q_{l\perp}\ , \tag{3.12}$$

such that

$$Q_{l\perp}\cdot p_\alpha=0=Q_{l\perp}\cdot p_\beta,\quad Q_{l\perp}^2=-q_{l\perp}^2$$

and

$$\begin{aligned} q_l^2&=-\alpha\beta s-q_{l\perp}^2\ ,\\ d^4q_l&=\tfrac{1}{2}|s|\,d\alpha\,d\beta\,d^2q_{l\perp}\ . \end{aligned} \tag{3.13}$$

The channel invariants are readily evaluated:

$$\begin{aligned} M_a^2&=(1-\alpha)\beta s-q_{l\perp}^2\ ,\\ M_b^2&=(1-\beta)\alpha s-q_{l\perp}^2\ ,\\ u_a&=-(1+\alpha)\beta s-(q_\perp-q_{l\perp})^2\ , \end{aligned} \tag{3.14}$$

where $q_\perp$ is the over-all transverse momentum transfer

$$p_a-p_{a'}\equiv Q\approx Q_\perp,\quad Q_\perp^2=-q_\perp^2\ . \tag{3.15}$$

The integration over loop momentum q_l would be carried out over all real α, β, and q_l except for the restrictions

$$\begin{aligned} &q_l^2\lesssim O(1)\ ,\\ &|M_a^2|\,|M_b^2|\lesssim|s|\delta\ , \end{aligned} \tag{3.16}$$

which require that

$$\begin{aligned} &|\beta|\,|\alpha|\lesssim\delta/|s|\ ,\\ &|q_{l\perp}^2+q_l^2|\lesssim\delta\ . \end{aligned} \tag{3.17}$$

The integral therefore has the form

$$\begin{aligned} \bar{A}_1(s,t)&=\int_D d^2q_{l\perp}\,\bar{H}(s,q_{l\perp},q_\perp)\ ,\\ \bar{H}(s,q_{l\perp},q_\perp)&=\bar{I}(s,q_{l\perp},q_\perp)\tfrac{1}{2}[(-s)^{\alpha_l}+\tau_l s^{\alpha_l}]\,\frac{\Gamma(-\alpha_l)}{t_u-m^2}\ , \end{aligned} \tag{3.18}$$

$$\bar{I}(s, q_{1\perp}, q_\perp) = \frac{-i}{(2\pi)^4}\int_D \tfrac{1}{2}|s|\, d\alpha\, d\beta \bar{B}_a(M_a{}^2, q_{1\perp}, q_\perp) \times \bar{B}_b(M_b{}^2, q_{1\perp}, q_\perp) ,$$

where we have assumed that δ is sufficiently small that the momentum transfers are entirely transverse:

$$t_1 = q_1{}^2 \approx -q_{1\perp}{}^2, \quad t \approx -q_\perp{}^2$$
$$t_u = q_u{}^2 \approx -(q_\perp - q_{1\perp})^2 . \tag{3.19}$$

In Appendix B we show that these approximations do not affect the J-plane decomposition and so are not essential.

To evaluate the asymptotic behavior of $\bar{A}_1(s, t)$ we evaluate its Mellin transform:

$$\bar{A}_1^\tau(J, t) = \frac{\Gamma(J+1)}{2\pi i}\int_0^\infty ds\, s^{-J-1}\, \mathrm{disc}\, \bar{A}_1^\tau(s, t) , \tag{3.20}$$

where

$$\mathrm{disc}\, \bar{A}_1^\tau(s, t) = \mathrm{disc}_+ \bar{A}_1(s, t) + \tau\, \mathrm{disc}_- \bar{A}_1(-s, t) , \tag{3.21a}$$

$$\bar{A}_1(s, t) = \tfrac{1}{2}\sum_\tau [\bar{A}_1^\tau(s, t) + \tau \bar{A}_1^\tau(-s, t)] \tag{3.21b}$$

defines the signatured amplitude so that its discontinuity is the usual sum or difference of the discontinuities across the right- and left-hand cuts of the amplitude $A_1(s, t)$. The inverse transform is then asymptotically

$$\bar{A}_1(s, t) \underset{s\to\infty}{\sim} \frac{1}{2\pi i}\int_C dJ\, \Gamma(-J) \sum_\tau \bar{A}_1^\tau(J, t) \times \tfrac{1}{2}[(-s)^J + \tau s^J] , \tag{3.22}$$

so that, for example, if

$$\bar{A}_1^{(+)}(J, t) \approx \frac{2}{\pi}\frac{\beta(t)}{J-1} \tag{3.23}$$

then

$$\bar{A}_1(s, t) \underset{s\to\infty}{\sim} i\beta(t) s . \tag{3.24}$$

To obtain $A_1^\tau(J, t)$ it is convenient first to transform $\bar{I}(s, q_{1\perp}, q_\perp)$ and then to correct for the Regge propagator in $\bar{H}(s, q_{1\perp}, q_\perp)$. The Mellin transform of $\bar{I}$ is much more straightforward, since without the Regge propagator, it is like the integral for the ordinary box graph. To obtain its Mellin transform, we must evaluate the discontinuities across right- and left-hand cuts in s, which are generated by the right- and left-hand poles and branch points in $\bar{B}_a$ and $\bar{B}_b$ as functions of $M_a{}^2$ and $M_b{}^2$. To study these, we write a dispersion relation (suppressing momentum-transfer arguments)

$$\bar{B}_a(M_a{}^2) = \frac{1}{2\pi i}\int_0^\infty du_a' \frac{\mathrm{disc}_- \bar{B}_a(u_a')}{u_a' - u_a - i\epsilon} + \frac{1}{2\pi i}\int_0^\infty d(M_a')^2 \frac{\mathrm{disc}_+ \bar{B}_a((M_a')^2)}{(M_a')^2 - (M_a)^2 - i\epsilon} , \tag{3.25}$$

and similarly for $\bar{B}_b$. (Subtractions may be included, if necessary.) Upon introducing the dispersion relation (3.25) for $\bar{B}_a$ and $\bar{B}_b$ into the integral for $\bar{I}$ (3.18), we find we must evaluate four integrals of the type

$$\tfrac{1}{2}\int |s|\, d\alpha\, d\beta \frac{1}{[M_a{}^2 - (M_a')^2 + i\epsilon]}\frac{1}{[M_b{}^2 - (M_b')^2 + i\epsilon]},$$
$$\tfrac{1}{2}\int |s|\, d\alpha\, d\beta \frac{1}{(u_a - u_a' + i\epsilon)}\frac{1}{[M_b{}^2 - (M_b')^2 + i\epsilon]} , \tag{3.26}$$

including two more with $M_b{}^2$ and $(M_b')^2$ replaced by u_b and u_b'. We treat them one by one and momentarily relax the constraint (3.17) to simplify the discussion.

For the first integral of (3.26), we see from (3.14) that if we integrate over β first the integral over α must be divided into the three domains

$$-\infty < \alpha < 0 ,$$
$$0 < \alpha < 1 , \tag{3.27}$$
$$1 < \alpha < \infty ,$$

to prevent singularities in $M_a{}^2$ and $M_b{}^2$ from crossing the real β axis. The integral over β can be evaluated explicitly using the residue theorem, since the poles in $M_a{}^2$ and $M_b{}^2$ produce poles in β on opposite sides of the contour. If they are on the same side, the integral over β is zero. Therefore, with (3.14) the first integral in (3.26) becomes

$$2\pi i\int_0^1 \frac{d\alpha}{2\alpha(1-\alpha)}\frac{1}{(M_{a'\perp})^2/(1-\alpha) + (M_{b'\perp})^2/\alpha - s} , \tag{3.28}$$

where

$$(M_{a'\perp})^2 = (M_a')^2 + q_{1\perp}{}^2 ,$$
$$(M_{b'\perp})^2 = (M_b')^2 + q_{1\perp}{}^2 . \tag{3.29}$$

The integral (3.28) has a branch point in s at

$$s = (M_{a'\perp} + M_{b'\perp})^2 . \tag{3.30}$$

When the integrations over q_1, $(M_a')^2$, and $(M_b')^2$ are taken into account, we see that the branch point (3.30) develops into the familiar right-hand branch point in s, and so we associate the branch point (3.30) with a right-hand discontinuity in s. The discontinuity of the cut in (3.28) is simply

$$(2\pi i)^2\int_0^1 \frac{d\alpha}{2\alpha(1-\alpha)}\,\delta\left(s-\frac{(M_a'_\perp)^2}{1-\alpha}-\frac{(M_b'_\perp)^2}{\alpha}\right)=(2\pi i)^2\,\tfrac{1}{2}|s|\int_0^1 d\alpha\int_0^1 d\beta\,\delta(M_a^2-(M_a')^2)\,\delta(M_b^2-(M_b')^2)\ . \quad (3.31)$$

When the integration over $(M_a')^2$ and $(M_b')^2$ is restored, we find that the right-hand cuts in $\bar{B}_a$ and $\bar{B}_b$ contribute

$$\mathrm{disc}_+\bar{I}(s)=\frac{-i}{(2\pi)^4}\,\tfrac{1}{2}|s|\int_0^1 d\alpha\int_0^1 d\beta\,\mathrm{disc}_+\bar{B}_a(M_a^2)\times\mathrm{disc}_+\bar{B}_b(M_b^2)\ . \quad (3.32)$$

Restoring the cutoff (3.17), we find for s positive

$$\alpha\beta\le\delta/s\ , \quad (3.33)$$

and since the minimum contributing value of M_a^2 or M_b^2 is $O(1)$, it follows that

$$\beta\le\delta\ ,\qquad \alpha\le\delta\ , \quad (3.34)$$

and

$$\beta\approx(M_a^2+q_{1\perp}^2)/s,\quad \alpha\approx(M_b^2+q_{1\perp}^2)/s\ , \quad (3.35)$$

and the integrals over α and β may be replaced by integrals over M_a^2 and M_b^2:

$$\mathrm{disc}_+\bar{I}(s)=\frac{-i}{(2\pi)^4}\,\frac{1}{2s}\int_D dM_a^2\,dM_b^2\,\mathrm{disc}_+\bar{B}_a(M_a^2)\times\mathrm{disc}_+\bar{B}_b(M_b^2)\ . \quad (3.36)$$

The contribution from the second integral of (3.26), arising from left-hand singularities in B_a and right-hand singularities in B_b, is readily evaluated with the same techniques. Owing to the relationship between u_a and the Sudakov variables (3.14), the integration over α is divided into the three domains

$$-\infty<\alpha<-1\ ,\qquad -1<\alpha<0\ ,\qquad 0<\alpha<\infty\ , \quad (3.37)$$

where only the region $-1<\alpha<0$ has poles on opposite sides of the β contour. The other regions give vanishing contributions to the integral. The integral over β yields

$$2\pi i\int_{-1}^0\frac{d\alpha}{2\alpha(1+\alpha)}\,\frac{1}{-s-u'_{a\perp}/(1+\alpha)+(M'_{b\perp})^2/\alpha}\ , \quad (3.38)$$

where

$$u'_{a\perp}=u'_a+(q_\perp-q_{1\perp})^2\ , \quad (3.39)$$

in analogy to (3.28) and (3.29) or, changing variables,

$$-2\pi i\int_0^1\frac{dx}{2x(1-x)}\,\frac{1}{s+u'_{a\perp}/x+(M'_{b\perp})^2/(1-x)} \quad (3.40)$$

It can be shown that when the $q_{1\perp}$ integration is taken into account, the branch point in s in (3.40) turns into the familiar u-channel normal threshold at

$$u=4m^2-s-t=[(u_a')^{1/2}+M_b']^2\ . \quad (3.41)$$

The discontinuity across this left-hand cut in s is

$$\mathrm{disc}_-\bar{I}(s,q_{1\perp})=\frac{-i}{(2\pi)^4}\,\frac{1}{2s}\int_D dM_a^2\,dM_b^2\,\mathrm{disc}_-\bar{B}_a(M_a^2,t,t_1)\times\mathrm{disc}_-\bar{B}_b(M_b^2,t,t_1)\ . \quad (3.42)$$

Discontinuities arising from the other two integrals analogous to (3.26) may be analyzed in a similar way, leading to the full discontinuities

$$i(2\pi)^4\,\mathrm{disc}_+\bar{I}(s)=\frac{1}{2s}\int_D dM_a^2\,dM_b^2\,(\mathrm{disc}_+\bar{B}_a)(\mathrm{disc}_-\bar{B}_b)+\frac{1}{2s}\int_D dM_a^2\,dM_b^2\,(\mathrm{disc}_-\bar{B}_a)(\mathrm{disc}_-\bar{B}_b), \quad (3.43)$$

$$i(2\pi)^4\,\mathrm{disc}_-\bar{I}(s)=\frac{1}{2s}\int_D dM_a^2\,dM_b^2\,(\mathrm{disc}_+\bar{B}_a)\,(\mathrm{disc}_-\bar{B}_b)+\frac{1}{2s}\int_D dM_a^2\,dM_b^2\,(\mathrm{disc}_-\bar{B}_a)\,(\mathrm{disc}_+\bar{B}_b).$$

(We have suppressed the transverse momentum arguments temporarily.)

Signature diagonalizes the discontinuity equations, as expected, so that

$$i(2\pi)^4\,\mathrm{disc}\,\bar{I}^\tau(s)=\frac{1}{2s}\int_{M_0^2}^{\delta s/M_0^2}dM_a^2\int_{M_0^2}^{\delta s/M_a^2}dM_b^2\,\mathrm{disc}\,\bar{B}_a^\tau(M_a^2)\,\mathrm{disc}\,\bar{B}_b^\tau(M_b^2)\ , \quad (3.44)$$

where the limits of integration are shown explicitly. This expression can be written in a form convenient for the Mellin transform:

$$i(2\pi)^4\,\mathrm{disc}\,\bar{I}^\tau(s)=\frac{1}{2s}\int_{1/\delta}^\infty d\lambda\int_{M_0^2}^\infty dM_a^2\int_{M_0^2}^\infty dM_b^2\,\delta(\lambda-s/M_a^2M_b^2)\,[\mathrm{disc}\,\bar{B}_a^\tau(M_a^2)]\,[\mathrm{disc}\,\bar{B}_b^\tau(M_b^2)]\ . \quad (3.45)$$

The Mellin transform may be obtained from the expression

$$i(2\pi)^4\int_1^\infty ds\, s^{-J-1}[\mathrm{disc}\, I^\tau(s)] = \tfrac{1}{2}\int_{1/\delta}^\infty \frac{d\lambda}{\lambda}\,\lambda^{-J-1}\int_{M_0^2}^\infty dM_a^{\,2}(M_a^{\,2})^{-J-1}[\mathrm{disc}\,\bar{B}_a^\tau(M_a^{\,2})] \times\int_{M_0^2}^\infty dM_b^{\,2}(M_b^{\,2})^{-J-1}[\mathrm{disc}\,\bar{B}_b^\tau(M_b^{\,2})]\ , \tag{3.46}$$

which separates to give

$$I^\tau(J, q_{1\perp}, q_\perp) = \frac{1}{16\pi^3\Gamma(J+1)}\,\bar{B}_a^\tau(J, q_{1\perp}, q_\perp) \times\frac{\delta^{J+1}}{J+1}\,\bar{B}_b^\tau(J, q_{1\perp}, q_\perp)\ , \tag{3.47}$$

where

$$\bar{B}_a^\tau(J, q_{1\perp}, q_\perp) = \frac{\Gamma(J+1)}{2\pi i}\int_{M_0^2}^\infty dM_a^{\,2}(M_a^{\,2})^{-J-1} \times \mathrm{disc}\,\bar{B}_a^\tau(M_a^{\,2}, q_{1\perp}, q_\perp)\ , \tag{3.48}$$

and similarly for $\bar{B}_b^\tau$.

In (3.47) and (3.48) we see the crucial importance of cuts in $M_a^{\,2}$ and $M_b^{\,2}$, without which no discontinuity in s would have appeared—therefore, no contribution to the Mellin transform. We state this result as a calculational rule:

Rule 1. For the purposes of calculating Mellin transforms of Reggeon diagrams, it suffices to keep only those parts of the loop integrals containing discontinuities in all cluster masses.

To find the Mellin transform of $H(s, q_{1\perp}, q_\perp)$ (3.18), which includes the Regge propagator, is a simple matter. We show in Appendix C that for positive signature $\tau_l = +$

$$\bar{H}^\tau(J, q_{1\perp}, q_\perp) = \bar{C}^\tau(J, \alpha_l)\,\bar{I}^\tau(J-\alpha_l, q_{1\perp}, q_\perp)\,\frac{\Gamma(-\alpha_l)}{t_u - m^2}\ ,$$

$$\bar{C}^{(+)}(J, \alpha_l) = \frac{\Gamma(-J+\alpha_l)}{\Gamma(-J)}\,\frac{\cos[\frac{1}{2}\pi(J-\alpha_l)]\cos(\frac{1}{2}\pi\alpha_l)}{\cos(\frac{1}{2}\pi J)}\ , \tag{3.49}$$

$$\bar{C}^{(-)}(J, \alpha_l) = \frac{\Gamma(-J+\alpha_l)}{\Gamma(-J)}\,\frac{\sin[\frac{1}{2}\pi(J-\alpha_l)]\cos(\frac{1}{2}\pi\alpha_l)}{\sin(\frac{1}{2}\pi J)}\ .$$

Inserting this expression into (3.18) and using (3.47) we obtain finally

$$\bar{A}_1^\tau(J, q_\perp) = \int\frac{d^2q_{1\perp}}{16\pi^3}\,\frac{\bar{C}^\tau(J, \alpha_l)}{\Gamma(J-\alpha_l+1)}\,\bar{B}_a^\tau(J-\alpha_l, q_{1\perp}, q_\perp) \times\frac{\delta^{J-\alpha_l+1}}{J-\alpha_l+1}\,\frac{\Gamma(-\alpha_l)}{(t_u-m^2)}\,\bar{B}_b^\tau(J-\alpha_l, q_{1\perp}, q_\perp)\ , \tag{3.50}$$

where $\alpha_l = \alpha_l(q_{1\perp}^{\,2})$ and $t_u = -(q_\perp - q_{1\perp})^2$ and according to (B25), $\bar{\delta} = \min[\delta, \lambda(t, t_l, t_u)/4t]$.

Whether a cut is actually present in $\bar{A}_1^\tau(J, q_\perp)$ depends on whether the integrand in (3.47) has a pole at $J = \alpha_l - 1$. The explicit pole is canceled by the Γ function. For positive signature $\bar{C}^{(+)}$ vanishes and $\bar{C}^{(-)}$ is finite at $J = \alpha_l - 1$. Therefore, if

$$\bar{N}_a^\tau(q_{1\perp}, q_\perp) = \lim_{J\to -1}(J+1)\,\bar{B}_a^\tau(J, q_{1\perp}, q_\perp)\ ,$$
$$\bar{N}_b^\tau(q_{1\perp}, q_\perp) = \lim_{J\to -1}(J+1)\,\bar{B}_b^\tau(J, q_{1\perp}, q_\perp) \tag{3.51}$$

are both finite for $\tau = +$ or either is finite for $\tau = -$ a cut appears in $\bar{A}_1^\tau(J)$. The coefficients $\bar{N}^\tau$ are commonly called the residues of the $J = -1$ fixed poles in $\bar{B}^\tau(J)$ and their presence reflects terms of the form

$$\bar{B}_a^\tau(M_a^{\,2}, q_{1\perp}, q_\perp) \sim \bar{N}_a^\tau(q_{1\perp}, q_\perp)/M_a^{\,2}\ ,$$
$$\bar{B}_b^\tau(M_b^{\,2}, q_{1\perp}, q_\perp) \sim \bar{N}_b^\tau(q_{1\perp}, q_\perp)/M_b^{\,2} \tag{3.52}$$

in the asymptotic behavior of the signatured amplitudes $\bar{B}_a^\tau(M_a^{\,2})$ and $\bar{B}_b^\tau(M_b^{\,2})$. Since we rule out such terms in the full amplitudes $\bar{B}_a(M_a^{\,2})$ and $\bar{B}_b(M_b^{\,2})$, it follows that

$$\bar{N}_a^{(-)} = 0 = \bar{N}_b^{(-)}\ . \tag{3.53}$$

In the standard jargon we allow only "nonsense-wrong-signature fixed poles." Therefore, there is a cut in $A_1^{(+)}(J, q_\perp)$ if *both* $N_a^{(+)}$ and $N_b^{(+)}$ are finite, but no cut in $A_1^{(-)}(J, q_\perp)$.

If the signature of the trajectory α_l had been negative the coefficients $\bar{C}^\tau$ would have been given instead by (C7) and the signatures of $\bar{B}_a^\tau$ and $\bar{B}_b^\tau$ in (3.50) would have been opposite to that of $\bar{A}_1^\tau$. Thus the pattern of poles and zeros in the expressions for $\bar{A}_1^{(+)}$ and $\bar{A}_1^{(-)}$ would have been reversed and we would have obtained a cut in $\bar{A}_1^{(-)}$ but not in $\bar{A}_1^{(+)}$. This result is a special case of a general rule[11] that the signature of a cut is the product of the signatures of the exchanged trajectories. (In this case there is only one exchanged trajectory.)

Returning to the case $\tau_l = +$, we may evaluate the discontinuity across the cut in $\bar{A}_1^{(+)}$ from (3.50), (3.49), and (3.51) with the result

$$\mathrm{disc}_J\bar{A}_1^{(+)}(J, q_\perp) = \int\frac{d^2q_{1\perp}}{16\pi^3}\,\frac{(2\pi i)}{\Gamma(-J)}\,\frac{\frac{1}{2}\pi\cos(\frac{1}{2}\pi\alpha_l)}{\cos(\frac{1}{2}\pi J)}\,\bar{N}_a^{(+)}(q_{1\perp}, q_\perp)\,\frac{\Gamma(-\alpha_l)}{t_u-m^2}\,\bar{N}_b^{(+)}(q_{1\perp}, q_\perp)\,\delta(J-\alpha_l+1)\ . \tag{3.54}$$

The net contribution to the asymptotic behavior from the cut is found from (3.22) to be

$$\bar{A}_1(s, q_\perp) \sim \int \frac{d^2 q_{1\perp}}{16\pi^3} \frac{1}{2} \pi \frac{\Gamma(-\alpha_l)\cos(\frac{1}{2}\pi\alpha_l)}{t_u - m^2} \bar{N}_a^{(+)}(q_{1\perp}, q_\perp) \bar{N}_b^{(+)}(q_{1\perp}, q_\perp) \exp[-i\tfrac{1}{2}\pi(\alpha_l - 1)] s^{\alpha_l - 1} . \tag{3.55}$$

The cut discontinuity is independent of the cutoff parameter δ. This can be traced to the fact that the cut arises from the high s, low M_a^2, M_b^2 portion of the integral (3.44), a region which is not influenced by the cutoff. On the other hand, $\bar{A}_1^\Gamma(J, q_\perp)$ develops poles in J where $\bar{B}_a^\Gamma$ and $\bar{B}_b^\Gamma$ have poles. The residues of these poles arise from the high M_a^2 and/or high M_b^2 part of the integral (3.44) where the cutoff operates. In this way the cutoff influences the renormalization of the poles in $\bar{B}_a^\Gamma$ and $\bar{B}_b^\Gamma$.

B. The two-Pomeron cut to lowest order

1. The evaluation of the Mellin transform

The analysis of the previous section makes possible the generalization to the lowest-order two-Pomeron-cut diagram of Fig. 13. If we proceed as before, examining the large-s behavior of the integrand before completing the loop integration, we face an apparent complication. When one of the Pomerons was replaced by a scalar particle, the asymptotic structure of the integrand could be deduced from a study of the six-point function before "sewing" it together. In the present case the structure of the whole integrand cannot be obtained in this way because, as we saw in example (3.6), the integrand must contain terms which do not factor into left and right amplitudes as the picture Fig. 13 would suggest. Nevertheless, we also saw that the only part of the integrand that contributed to the Mellin transform was the part containing discontinuities in M_a^2 and M_b^2, and this part of the integrand did indeed factor into left and right amplitudes. So there is no problem after all.

The structure of that part of the integrand containing M_a^2 and M_b^2 discontinuities can be obtained by writing a dispersion relation in M_a^2 and M_b^2. The discontinuity in the dispersion relation is associated with on-mass-shell states as indicated in Fig. 14. Interchanging the asymptotic limit $s \to \infty$ with the integration over the intermediate momenta leads to the usual Regge asymptotic limit on 2-n scattering amplitudes. Completing the integration over intermediate states and the dispersion integrals then yields the expression

$$A_1(s,t) = \frac{-i}{(2\pi)^4} \int_D d^4 q_l \, B_a(M_a^2, t, t_l, t_u) \frac{\Gamma(-\alpha_l)}{2} [(-s)^{\alpha_l} + \tau_l s^{\alpha_l}]$$

$$\times \frac{\Gamma(-\alpha_u)}{2} [(-s)^{\alpha_u} + \tau_u s^{\alpha_u}] B_b(M_b^2, t, t_l, t_u) , \tag{3.56}$$

which is analogous to (3.9).

The amplitude B_a is that part of the two-Pomeron, two-particle scattering amplitude which has a discontinuity in M_a^2. It also appears in the helicity asymptotic limit of the six-particle amplitude of Fig. 15:

$$T_6 \sim B_a(M_a^2, t, t_u, t_l) \frac{\Gamma(-\alpha_l)}{2} [(-s_l)^{\alpha_l} + \tau_l s_l^{\alpha_l}] \frac{\Gamma(-\alpha_u)}{2} [(-s_u)^{\alpha_u} + \tau_u s_u^{\alpha_u}] \beta_{cd}(t_l) \beta_{c'd'}(t_u)$$

$$+ \text{other terms}, \tag{3.57}$$

where the definition of invariants is the same as in the left half of Fig. 11, except for s_u and s_l as shown in Fig. 15; β_{cd} and $\beta_{c'd'}$ are the two-particle-Pomeron residue factors and the "other terms" are entire in M_a^2. The inclusive cross section is given by the Mueller discontinuity[28] of T_6 in the special case $(a, c, d) \equiv (a', c', d')$, $t = 0$, $t_u = t_l$, $s_u = s_l = s$, $\alpha_l = \alpha_u = \alpha$, $\tau_l = \tau_u = \tau$ by

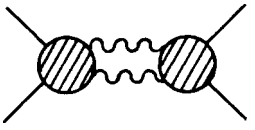

FIG. 13. Lowest-order two-Pomeron-cut diagram.

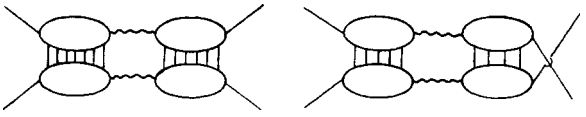

FIG. 14. Contribution to dispersion relations in M_a^2 and M_b^2.

$$\frac{d\sigma^{ac\to d}}{dt_l dM_a^{\,2}} \underset{s\to\infty}{\sim} \frac{1}{16\pi s^2}\,\frac{\mathrm{disc}B_a(M_a^{\,2},0,t_l,t_l)}{2\pi i}\,|\xi_\tau|^2\,, \tag{3.58}$$

where

$$\xi_+ = \Gamma(-\alpha)\cos(\tfrac{1}{2}\pi\alpha)$$

and

$$\xi_- = -i\Gamma(-\alpha)\sin(\tfrac{1}{2}\pi\alpha)\,,$$

which is valid for $M_a^{\,2} \ll s$; i.e., from the two-body region up to the triple-Regge region.[29] [The two-body cross section $ac \to bd$ is obtained by setting $\mathrm{disc}B_a = 2\pi i\delta(M_a^{\,2} - m_a^{\,2})\beta_{ab}^{\,2}(t)$.]

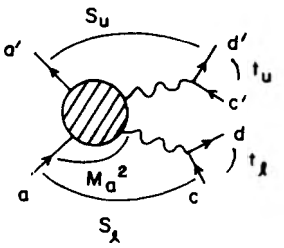

FIG. 15. Six-particle amplitude.

The remaining analysis of the J-plane projection of the two-Pomeron-cut diagram proceeds just as before with only slight changes due to the extra Regge propagator. The Mellin transform of (3.56) is

$$A_1^\tau(J,q_\perp) = \Gamma(J+1)\int \frac{d^2q_{l\perp}}{16\pi^3}\,\frac{B_a^\tau(J-\alpha_l-\alpha_u,q_\perp,q_{l\perp})}{\Gamma(J-\alpha_l-\alpha_u+1)} \times \frac{\zeta^\tau(J,\alpha_l,\alpha_u)\Gamma(-\alpha_l)\Gamma(-\alpha_u)\bar\delta^{J-\alpha_l-\alpha_u+1}}{(J-\alpha_l-\alpha_u+1)\Gamma(J-\alpha_l-\alpha_u+1)} B_b^\tau(J-\alpha_l-\alpha_u,q_\perp,q_{l\perp}), \tag{3.59}$$

where $q_{l\perp}+q_{u\perp}=q_\perp$, $\alpha_l=\alpha_l(q_{l\perp}^{\,2})$, and $\alpha_u=\alpha_u(q_{u\perp}^{\,2})$. The cutoff $\bar\delta$ is given by (B25) to be $\min[\delta,\lambda(t,t_l,t_u)/4t]$, and for even signature ($\tau_u=\tau_l=+$)

$$\zeta^{(+)}(J,\alpha_l,\alpha_u) = \frac{\sin(\frac{1}{2}\pi J)\cos(\frac{1}{2}\pi\alpha_l)\cos(\frac{1}{2}\pi\alpha_u)}{\sin[\frac{1}{2}\pi(J-\alpha_l-\alpha_u)]}\,, \tag{3.60}$$

$$\zeta^{(-)}(J,\alpha_l,\alpha_u) = \frac{\cos(\frac{1}{2}\pi J)\cos(\frac{1}{2}\pi\alpha_l)\cos(\frac{1}{2}\pi\alpha_u)}{\cos[\frac{1}{2}\pi(J-\alpha_l-\alpha_u)]}\,,$$

$$B_{a,b}^\tau(J,q_\perp,q_{l\perp}) = \frac{\Gamma(J+1)}{2\pi i}\int_0^\infty dM^2(M^2)^{-J-1} \times \mathrm{disc}B_{a,b}^\tau(M^2,q_\perp,q_{l\perp})\,. \tag{3.61}$$

[The factor $\zeta^\tau(J,\alpha_l,\alpha_u)$ does not, in fact, introduce singularities into the partial-wave amplitude, since to avoid right-signature fixed poles, both B_a^τ and B_b^τ must vanish at the zeros of the denominator of ζ^τ.]

As before the cut appears only in the positive-signatured amplitude if $\tau_l=\tau_u=+$. Its discontinuity is

$$\mathrm{disc}_J A_1^{(+)}(J,q_\perp) = \int \frac{d^2q_{l\perp}}{16\pi^3}\,\frac{1}{2}\,\pi\,\frac{\Gamma(-\alpha_l)\cos(\frac{1}{2}\pi\alpha_l)\Gamma(-\alpha_u)\cos(\frac{1}{2}\pi\alpha_u)}{\Gamma(-J)\cos(\frac{1}{2}\pi J)} \times N_a^{(+)}(q_\perp,q_{l\perp})N_b^{(+)}(q_\perp,q_{l\perp})2\pi i\delta(J-\alpha_l-\alpha_u+1)\,, \tag{3.62}$$

where the residues of the fixed poles are

$$N_{a,b}^\tau(q_\perp,q_{l\perp}) \equiv \lim_{J\to -1}(J+1)B_{a,b}^\tau(J,q_\perp,q_{l\perp})\,. \tag{3.63}$$

The cut discontinuity is evidently independent of the cutoff parameter $\bar\delta$ as before.

2. *Comparison with two-component model*

It is useful to compare the result for the two-Pomeron cut obtained in the Reggeon calculus with the result calculated using the traditional multi-

peripheral two-component model (see, for example, Abarbanel[30]). The latter model deals strictly with the s-channel absorptive part of the 2-2 amplitude, and although it gives the wrong sign for the cut, it calculates, nonetheless, a physical contribution to the total cross section, which is attributed to those events with one large rapidity gap.

When working with absorptive parts, it is convenient to use a modified form of the Mellin transform:

$$\mathfrak{A}(J)=\int ds\,\frac{1}{2i}\,[\mathrm{disc}A(s)]s^{-J-1}\,, \tag{3.64a}$$

$$\frac{1}{2i}\,\mathrm{disc}A(s)=\frac{1}{2\pi i}\int dJ\,\mathfrak{A}(J)s^{J}\,, \tag{3.64b}$$

where the connection with the full transform (3.20) is

$$\mathfrak{A}(J)=\frac{\pi}{2\Gamma(J+1)}\,[A^{(+)}(J)+A^{(-)}(J)]\,. \tag{3.65}$$

In these expressions $\mathrm{disc}A(s)$ refers to the discontinuity across the right-hand cut only.

The large gap processes contribute to the forward elastic absorptive part

$$\frac{1}{2i}\,\mathrm{disc}A_1(s,0)_{\mathrm{gap}}=\frac{2}{(2\pi)^4}\int_D d^2q_{1\perp}dM_a{}^2dM_b{}^2\left[\frac{1}{2i}\,\mathrm{disc}B_a(M_a{}^2,0,q_{1\perp})\right]\left[\frac{1}{2i}\,\mathrm{disc}B_b(M_b{}^2,0,q_{1\perp})\right]$$
$$\times|\Gamma(-\alpha_1)\exp(-i\tfrac{1}{2}\pi\alpha_1)\cos(\tfrac{1}{2}\pi\alpha_1)|^2s^{2\alpha_1-1}\,, \tag{3.66}$$

where the cutoff criterion is exactly as before. The Mellin transform is then

$$\mathfrak{A}_1(J,0)_{\mathrm{gap}}=\frac{2}{(2\pi)^4}\int d^2q_{1\perp}\mathfrak{B}_a(J-2\alpha_1,0,q_{1\perp})\times\frac{\bar{\delta}^{J-2\alpha_1+1}[\Gamma(-\alpha_1)\cos(\frac{1}{2}\pi\alpha_1)]^2}{J-2\alpha_1+1}\times\mathfrak{B}_b(J-2\alpha_1,0,q_{1\perp})\,, \tag{3.67}$$

in agreement with Abarbanel.[30] The two-Pomeron amplitudes B_a and B_b are necessarily even under crossing and the large gap cross section is the same for the crossed processes so that $A_{1,\mathrm{gap}}(s)$ is also even. Therefore, using Eq. (3.65) with negative-signatured amplitudes identically zero, we can cast the full amplitude from the Reggeon calculus (3.59) in a form which can be compared with (3.67). We find from (3.59) in the forward direction that the full contribution to the absorptive part is

$$\mathfrak{A}_1(J,0)=\frac{2}{(2\pi)^4}\int d^2q_{1\perp}\mathfrak{B}_a(J-2\alpha_1,0,q_{1\perp})\frac{\bar{\delta}^{J-2\alpha_1+1}[\Gamma(-\alpha_1)\cos(\frac{1}{2}\pi\alpha_1)]^2}{J-2\alpha_1+1}\,\frac{\sin(\frac{1}{2}\pi J)}{\sin[\frac{1}{2}\pi(J-2\alpha_1)]}\,\mathfrak{B}_b(J-2\alpha_1,0,q_{1\perp})\,. \tag{3.68}$$

The only difference is the ratio of sine functions, which for $J\approx 1$, $\alpha_1\approx 1$ reverses the sign. It is also noteworthy that a measurement of the large gap cross section at various $M_a{}^2$, $M_b{}^2$, and $t_1=-q_{1\perp}{}^2$ and knowledge of $\alpha_1(t_1)$ permit an exact computation of the full amplitude (3.68) in the forward direction.

The expressions (3.67) and (3.68) may be readily generalized away from the forward direction.

3. *Contribution to the total cross section*

Expression (3.68) together with (3.64a) gives two types of contributions to the total cross section. One comes from the cut and the other from double poles due to Regge poles in B_a and B_b. The cut discontinuity is

$$\mathrm{disc}_J\mathfrak{A}_1(J,0)=\int\frac{d^2q_{1\perp}}{32\pi^2}\,N_a^{(+)}(0,q_{1\perp})N_b^{(+)}(0,q_{1\perp})[\Gamma(-\alpha_1)\cos(\tfrac{1}{2}\pi\alpha_1)]^2\cos\pi\alpha_1(2\pi i)\delta(J-2\alpha_1+1)\,, \tag{3.69}$$

where $N^{\tau}_{a,b}$ are given by (3.63), giving a contribution to the total cross section

$$\sigma_{1,\mathrm{cut}}(s)\underset{s\to\infty}{\sim}\int\frac{d^2q_{1\perp}}{32\pi^2}\,N_a^{(+)}(0,q_{1\perp})N_b^{(+)}(0,q_{1\perp})[\Gamma(-\alpha_1)\cos(\tfrac{1}{2}\pi\alpha_1)]^2\cos\pi\alpha_1 s^{2\alpha_1-2}\,. \tag{3.70}$$

The factor $\cos\pi\alpha_l$ makes the contribution negative for $\alpha_l \simeq 1$, a famous result.[31] If it had been omitted, we would have obtained the contribution to the total cross section from events with one large rapidity gap.

A Regge pole at $J=\alpha_0$ in $B_a^{\tau_0}(J-\alpha_l-\alpha_u)$ corresponds to the asymptotic behavior

$$B_a(M_a^2, q_\perp, q_{l\perp}) \underset{M_a^2\to\infty}{\sim} \beta_a(t)\Gamma(-\alpha_0+\alpha_l+\alpha_u)\tfrac{1}{2}[(-M_a^2)^{\alpha_0-\alpha_l-\alpha_u}+\tau_0\tau_l\tau_u(M_a^2)^{\alpha_0-\alpha_l-\alpha_u}]\,\gamma(t,t_l,t_u)\,. \tag{3.71}$$

Corresponding to this behavior is a pole in the J plane

$$B_a^{\tau_0}(J-\alpha_l-\alpha_u, q_{l\perp}, q_\perp) \approx \frac{\beta_a(t)\gamma(q_{l\perp}, q_\perp)}{J-\alpha_0}\,, \tag{3.74}$$

and similarly for $B_b^{\tau_0}$. Together they produce a double pole in $\mathfrak{A}_1(J,0)$ so that from (3.68)

$$\mathfrak{A}_1(J,0) \approx \frac{1}{(J-\alpha_0)^2}\beta_a(0)\beta_b(0)G(0)\,, \tag{3.75}$$

where

$$G(t) = \int \frac{d^2q_{l\perp}}{8\pi^2}\frac{\Gamma(-\alpha_l)\cos(\frac{1}{2}\pi\alpha_l)\Gamma(-\alpha_u)\cos(\frac{1}{2}\pi\alpha_u)\bar{\delta}^{\alpha_0-\alpha_l-\alpha_u+1}\sin(\frac{1}{2}\pi\alpha_0)}{\sin[\frac{1}{2}\pi(\alpha_0-2\alpha_l)]\,(\alpha_0-\alpha_l-\alpha_u+1)}\,\bar{\gamma}^2(q_{l\perp}, q_\perp)\,. \tag{3.76}$$

In terms of these factors the inclusive cross section (3.58) for $\tau_l=\tau_u=\tau$ and $\tau_0=+$ has the triple-Regge behavior[29]

$$\frac{d\sigma^{ac\to d}}{dt_l dM_a^2} \underset{\substack{M^2\to\infty\\ s/M^2\to\infty}}{\sim} \frac{1}{16\pi}\beta_a(0)\bar{\gamma}(0,t_l,t_l)|\xi_\tau|^2(M_a^2)^{\alpha_0-2\alpha}s^{2\alpha-2}\,, \tag{3.72}$$

where

$$\bar{\gamma}(t,t_u,t_l) = \frac{\gamma(t,t_u,t_l)}{2\Gamma(1+\alpha_0-\alpha_l-\alpha_u)}\,. \tag{3.73}$$

(There is also a single pole at $J=\alpha_0$ arising from the interference of the pole in B_a with background in B_b and vice versa.) Such a double pole produces an asymptotic contribution to the total cross section

$$\sigma_{1,\text{pole}} \sim \beta_a(0)\beta_b(0)G(0)s^{\alpha_0}\ln s\,. \tag{3.77}$$

If $\alpha_l \approx 1$ over most of the range of significant contribution to the integral (3.76) then $G(0)=C/(1-\alpha_0)$, where C is positive. In such a case the contribution of the double pole to the total cross section is positive when $\alpha_0<1$ and negative when $\alpha_0>1$. The contribution when α_0 coincides with the cut cannot be calculated independently of the cut contribution (3.70) in general since N_a and N_b are singular when G is singular. [The exception occurs when $\bar{\gamma}$ vanishes with the denominator in (3.76).]

C. Higher-order contributions to the two-Reggeon cut

1. *Reggeon-particle cuts*

Since some new complications arise in treating the higher-order contributions, we first discuss the simpler diagram of Fig. 16, which is obtained by "sewing" together the eight-particle amplitude shown. Because of the cutoff criteria

$$\begin{aligned} &\delta|s_1| \gtrsim |M_a^2||M^2|\,,\quad \delta|s| \gtrsim |M_a^2||s_2|\,,\\ &\delta|s_2| \gtrsim |M_b^2||M^2|\,,\quad \delta|s| \gtrsim |M_b^2||s_1|\,, \end{aligned} \tag{3.78}$$

we seek an expression for the eight-particle amplitude with s_1, s_2, and s large. In this limit the amplitude has a form which resembles the expression of Sec. III A for the five-particle amplitude (3.6) in that there are several leading terms controlled by the trajectories in t_a, t_b, t_{1l}, t_{2l}, and t. However, only two of these terms have singularities simultaneously in M_a^2, M_b^2, and M^2, namely

$$\begin{aligned} T_8 \sim\ & \bar{B}_a(M_a^2; t_a, t_{1l}, t_{1u})\bar{B}_2(M^2; t_{1u}, t_{1l}, t_{2u}, t_{2l})\,\bar{B}_b(M_b^2; t_b, t_{2u}, t_{2l})\\ &\times\Gamma(-\alpha_1)\tfrac{1}{2}[(-s_1)^{\alpha_1-\alpha_2}+\tau_1\tau_2 s_1^{\alpha_1-\alpha_2}]\,\tfrac{1}{2}[(-s)^{\alpha_2}+\tau_2 s^{\alpha_2}]\Gamma(-\alpha_2)\\ &+\bar{B}_a(M_a^2; t_a, t_{1l}, t_{1u})\bar{B}_1(M^2; t_{1u}, t_{1l}, t_{2u}, t_{2l})\bar{B}_b(M_b^2, t_b, t_{2u}, t_{2l})\\ &\times\Gamma(-\alpha_1)\tfrac{1}{2}[(-s)^{\alpha_1}+\tau_1 s^{\alpha_1}]\,\tfrac{1}{2}[(-s_2)^{\alpha_2-\alpha_1}+\tau_1\tau_2 s_2^{\alpha_2-\alpha_1}]\Gamma(-\alpha_2)\,, \end{aligned} \tag{3.79}$$

where $\alpha_1=\alpha_1(t_{1l})$, $\alpha_2=\alpha_2(t_{2l})$. As before, we shall find that only this part of T_8 contributes to the Mellin transform of the diagram. Factorization of the Pomeron residue makes possible the separation of the factors B_a, B_1, B_2, and B_b. Except for the dependence on a few extra variables, the structure of (3.79) is identical to that of a five-particle amplitude in the double-Regge limit.

The evaluation of the Mellin transform of the amplitude corresponding to Fig. 16, namely,

$$A_2(s,t)=\frac{-1}{(2\pi)^8}\int_D d^4q_{1l}\,d^4q_{2l}\,T_8\,\frac{1}{t_{1u}-m^2}\,\frac{1}{t_{2u}-m^2}\ , \tag{3.80}$$

can be copied from Sec. IIIA, if the integral is performed by first combining two of the bubbles of Fig. 16 into a single bubble and letting s_1 (or s_2) play the role of a cluster mass. [The factor $-(2\pi)^{-8}$ gives a positive imaginary part to A_2 in the forward direction if $\alpha_{1l}=\alpha_{1u}=\alpha_{2l}=\alpha_{2u}\equiv 0$ and the B's all have positive imaginary parts themselves.] Because of the structure of the two terms of T_8 (3.79), it is natural to treat the integral over the first term and second term in different ways, and so it is natural to integrate the first term, treating s_1 as a single cluster mass. The second term is integrated the other way, treating s_2 as a single cluster mass. We define, therefore, (suppressing momentum-transfer arguments)

$$\begin{aligned}
D_a(s_1)&=\frac{-i}{(2\pi)^4}\int_D d^4q_{1l}\,\bar B_a(M_a{}^2)\Gamma(-\alpha_1)\tfrac{1}{2}[(-s_1)^{\alpha_1-\alpha_2}+\tau_1\tau_2 s_1{}^{\alpha_1-\alpha_2}]\bar B_2(M^2)\ ,\\
D_b(s_2)&=\frac{-i}{(2\pi)^4}\int_D d^4q_{2l}\,\bar B_1(M^2)\Gamma(-\alpha_2)\tfrac{1}{2}[(-s_2)^{\alpha_2-\alpha_1}+\tau_1\tau_2 s_2{}^{\alpha_2-\alpha_1}]\bar B_b(M_b{}^2)\ .
\end{aligned} \tag{3.81}$$

The amplitude $A_2(s,t)$ is then

$$\begin{aligned}
A_2(s,t)=&\frac{-i}{(2\pi)^4}\int_D d^4q_{2l}\,\bar D_a(s_1)\frac{\Gamma(-\alpha_2)}{t_{2u}-m^2}\,\tfrac{1}{2}[(-s)^{\alpha_2}+\tau_2 s^{\alpha_2}]\bar B_b(M_b{}^2)\\
&+\frac{-i}{(2\pi)^4}\int_D d^4q_{1l}\,\bar B_a(M_a{}^2)\frac{\Gamma(-\alpha_1)}{t_{1u}-m^2}\,\tfrac{1}{2}[(-s)^{\alpha_1}+\tau_1 s^{\alpha_1}]\bar D_b(s_2)\ ,
\end{aligned} \tag{3.82}$$

which is identical in structure to (3.9). The Mellin transform follows directly from (3.50):

$$\begin{aligned}
\bar A_2{}^\tau(J,q_\perp)=&\int_D\frac{d^2q_{2\perp}}{16\pi^3}\,\frac{\bar C^\tau(J,\alpha_2)}{\Gamma(J-\alpha_2+1)}\,\frac{\Gamma(-\alpha_2)}{t_{2u}-m^2}\,\bar D_a{}^\tau(J-\alpha_2,q_\perp,q_{2\perp})\frac{\bar\delta_2{}^{J-\alpha_2+1}}{J-\alpha_2+1}\,\bar B_b{}^\tau(J-\alpha_2,q_\perp,q_{2\perp})\\
&+\int\frac{d^2q_{1\perp}}{16\pi^3}\,\frac{\bar C^\tau(J,\alpha_1)}{\Gamma(J-\alpha_1+1)}\,\frac{\Gamma(-\alpha_1)}{t_{1u}-m^2}\,\bar B_a{}^\tau(J-\alpha_1,q_\perp,q_{1\perp})\frac{\bar\delta_1{}^{J-\alpha_1+1}}{J-\alpha_1+1}\,\bar D_b{}^\tau(J-\alpha_1,q_\perp,q_{1\perp})\ ,
\end{aligned} \tag{3.83}$$

where $q_{1\perp}$ and $q_{2\perp}$ are the components of q_{1l} and q_{2l} transverse to p_a and p_b. The Mellin transforms of $\bar D_a(s_1)$ and $\bar D_b(s_2)$, which appear in (3.83), can be evaluated in turn using the same procedure, since the integrals (3.81) have nearly the same structure. The chief difference here is that the four-momentum q_1 or q_2 appears as an external variable in place of p_a or p_b. In defining the Sudakov variables, we find it most convenient to continue to use the momenta p_a and p_b as basis vectors. The kinematics analogous to that in the discussion of Eqs. (3.14) through (3.47) is only slightly modified, and we find

$$\begin{aligned}
\bar D_a{}^\tau(J,q_\perp,q_{2\perp})=&\int\frac{d^2q_{1\perp}}{16\pi^3}\,\frac{\bar C^\tau(J,\alpha_1-\alpha_2)}{\Gamma(J-\alpha_1+\alpha_2-1)}\,\bar B_a{}^\tau(J-\alpha_1+\alpha_2,q_\perp,q_{1\perp})\frac{\bar\delta_1{}^{J-\alpha_1+\alpha_2-1}}{J-\alpha_1+\alpha_2-1}\\
&\times\bar B_2{}^\tau(J-\alpha_1+\alpha_2,q_\perp,q_{1\perp},q_{2\perp})\ ,\\
\bar D_b{}^\tau(J,q_\perp,q_{1\perp})=&\int\frac{d^2q_{2\perp}}{16\pi^3}\,\frac{\bar C^\tau(J,\alpha_2-\alpha_1)}{\Gamma(J-\alpha_2+\alpha_1-1)}\,\bar B_1(J-\alpha_2+\alpha_1,q_\perp,q_{1\perp},q_{2\perp})\frac{\bar\delta_2{}^{J-\alpha_2+\alpha_1-1}}{J-\alpha_2+\alpha_1-1}\\
&\times\bar B_b{}^\tau(J-\alpha_2+\alpha_1,q_\perp,q_{2\perp})\ .
\end{aligned} \tag{3.84}$$

Inserting these expressions into (3.83) then gives the final result

$$\begin{aligned}
\bar A_2{}^\tau(J,q_\perp)=&\int\frac{d^2q_{1\perp}d^2q_{2\perp}}{(16\pi^3)^2}\,\bar B_a{}^\tau(J-\alpha_1,q_\perp,q_{1\perp})\,\frac{\Gamma(-\alpha_1)}{t_{1u}-m^2}\\
&\times\frac{\bar\delta_1{}^{J-\alpha_1+1}}{J-\alpha_1+1}\left[\frac{\bar B_2{}^\tau(J-\alpha_1,q_\perp,q_{1\perp},q_{2\perp})}{\Gamma(J-\alpha_2+1)\Gamma(J-\alpha_1+1)}\,\bar C^\tau(J,\alpha_2)\bar C^\tau(J-\alpha_2,\alpha_1-\alpha_2)\right.\\
&\left.+\frac{\bar B_1{}^\tau(J-\alpha_2,q_\perp,q_{1\perp},q_{2\perp})}{\Gamma(J-\alpha_1+1)\Gamma(J-\alpha_2+1)}\,\bar C^\tau(J-\alpha_1,\alpha_2-\alpha_1)\bar C^\tau(J,\alpha_1)\right]\\
&\times\frac{\bar\delta_2{}^{J-\alpha_2+1}}{J-\alpha_2+1}\,\frac{\Gamma(-\alpha_2)}{t_{2u}-m^2}\,\bar B_b{}^\tau(J-\alpha_2,q_\perp,q_{2\perp})\ .
\end{aligned} \tag{3.85}$$

A J-plane cut is generated from poles in the integrand at $J=\alpha_1-1$ and $J=\alpha_2-1$. A net pole occurs at $J=\alpha_1-1$ if B_a^τ has a fixed pole and either B_2^τ has a fixed pole or B_1^τ does not vanish.

2. *Factorization and the iteration of the Reggeon-particle cut*

If this expression is compared with the previous result for the lowest-order Reggeon-particle-cut diagram (3.50), it is possible to identify the terms in the factorized expression

$$\bar{A}_1^\tau(J,q_\perp)=K^\tau(J)\int\frac{d^2q_{1\perp}}{16\pi^3}\,\bar{B}_a^\tau(J,q_\perp,q_{1\perp})\bar{P}_1(J,q_\perp,q_{1\perp})\bar{B}_b^\tau(J,q_\perp,q_{1\perp})\,,$$
$$\bar{A}_2^\tau(J,q_\perp)=K^\tau(J)\int\frac{d^2q_{1\perp}d^2q_{2\perp}}{(16\pi^3)^2}\,\bar{B}_a^\tau(J,q_\perp,q_{1\perp})\bar{P}_1(J,q_\perp,q_{1\perp})\bar{B}^\tau(J,q_\perp,q_{1\perp},q_{2\perp})\bar{P}_2(J,q_\perp,q_{2\perp})\bar{B}_b^\tau(J,q_\perp,q_{2\perp})\,. \tag{3.86}$$

The Reggeon-particle amplitudes are illustrated in Fig. 17. The term K is a normalization factor, and P_i is a propagator for the particle and Pomeron. The diagrams of Fig. 17 serve equally well to represent the momentum space and the J-plane construction of the amplitudes.

For $\tau=+$ and a positive-signatured Reggeon we find in comparing (3.86) with (3.50) and (3.85) that

$$K_*^{(+)}(J)=\frac{1}{\Gamma(-J)\cos(\frac{1}{2}\pi J)}\,,$$
$$\bar{P}_i^{(+)}=\frac{\Gamma(-\alpha_i)}{t_{iu}-m^2}\times\frac{\Gamma(-J+\alpha_i)\cos[\frac{1}{2}\pi(J-\alpha_i)](\cos\frac{1}{2}\pi\alpha_i)\bar{\delta}_i^{J-\alpha_i+1}}{\Gamma(J-\alpha_i+1)(J-\alpha_i+1)}\,, \tag{3.87}$$
$$\bar{B}^{(+)}(J)=\frac{\cos[\frac{1}{2}\pi(\alpha_1-\alpha_2)]}{(\cos\frac{1}{2}\pi\alpha_1)}\frac{\bar{B}_2^\tau(J-\alpha_1)}{\Gamma(-J+\alpha_2)\cos[\frac{1}{2}\pi(J-\alpha_2)]}+\frac{\cos[\frac{1}{2}\pi(\alpha_2-\alpha_1)]}{(\cos\frac{1}{2}\alpha_2)}\frac{\bar{B}_1^\tau(J-\alpha_2)}{\Gamma(-J+\alpha_1)\cos[\frac{1}{2}\pi(J-\alpha_1)]}\,.$$

As a consistency check, one can next treat the diagram of Fig. 18 which has more terms of the type shown in (3.79)—five, to be exact. If we use factorization techniques discussed by Weis,[32] for the 2-4 amplitude, it is possible to show after considerable labor that the Mellin transform is given correctly by

$$\bar{A}_3=K\int\frac{d^2q_{1\perp}d^2q_{2\perp}d^2q_{3\perp}}{(16\pi^3)^3}\,\bar{B}_a\bar{P}_1\bar{B}\bar{P}_2\bar{B}\bar{P}_3\bar{B}_b\,, \tag{3.88}$$

in agreement with (3.86) and (3.87). We would not be rash in concluding that further iterations of the Reggeon-particle cut should also factor in this way.

With these results it is straightforward to derive an integral equation for the sum of all iterations of the Pomeron-particle cut, although we advise against taking it too seriously as a realistic representation for the four-particle amplitude since many diagrams have yet to be included. Following the symbolic notation of (3.88) we write

$$\bar{A}=\sum_n\bar{A}_n=K\int\frac{d^2q_{1\perp}}{16\pi^3}\,\bar{U}_1\bar{P}_1\bar{B}_b\,,$$
$$\bar{U}_1=\bar{B}_a+\int\frac{d^2q_{2\perp}}{16\pi^3}\,\bar{U}_2\bar{P}_2\bar{B}\,, \tag{3.89}$$

where

$$\bar{U}_i\equiv\bar{U}^\tau(J,q_\perp,q_{i\perp})\,.$$

3. *Two-Reggeon cuts*

The analysis of the two-Reggeon-cut diagram of Fig. 19 presents a further difficulty. When one Reggeon in each link was replaced by a scalar particle in the previous subsection, the Regge propagators appeared in the form [see (3.79)]

$$R_{1,2}=\tfrac{1}{2}[(-s_1)^{\alpha_1-\alpha_2}+\tau_1\tau_2 s_1^{\alpha_1-\alpha_2}]\times\tfrac{1}{2}[(-s)^{\alpha_2}+\tau_2 s^{\alpha_2}]\,,$$
$$R_{2,1}=\tfrac{1}{2}[(-s_2)^{\alpha_2-\alpha_1}+\tau_1\tau_2 s_2^{\alpha_2-\alpha_1}]\times\tfrac{1}{2}[(-s)^{\alpha_1}+\tau_1 s^{\alpha_1}]\,. \tag{3.90}$$

Because the singularities of the propagators in s_1

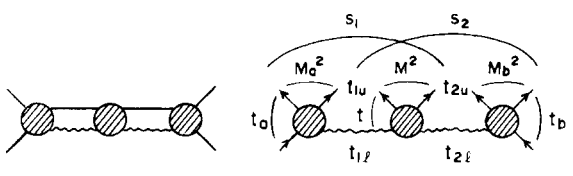

FIG. 16. First iteration of the Reggeon-particle-cut diagram and associated integrand with notation.

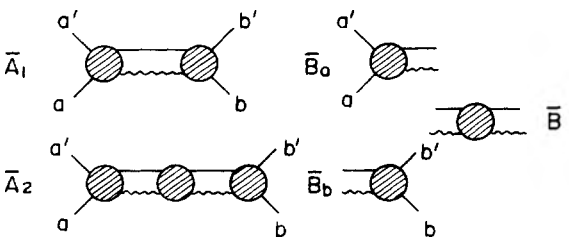

FIG. 17. Amplitudes for constructing Reggeon graphs.

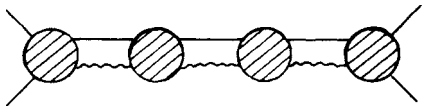

FIG. 18. Higher-order Reggeon-particle-cut diagram.

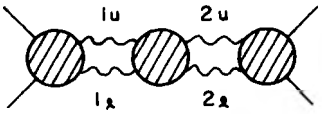

FIG. 19. First iteration of the two-Reggeon cut.

and s_2 were additive in (3.79), it was possible to select an order of integration which permitted the s_1 dependence, or s_2 dependence, of the propagator to be factored, so that the results of the singularity analysis of Sec. III A could be applied. In the present case the integrand must contain a product of two sets of such propagators. Thus (with momentum-transfer arguments suppressed)

$$A_2(s) = \frac{-1}{(2\pi)^8}\int d^4q_1 d^4q_2 B_a(M_a^2)\Gamma(-\alpha_{1l})\Gamma(-\alpha_{1u}) \times [B_{22}(M^2)R_{1l,2l}R_{1u,2u} + B_{21}(M^2)R_{1l,2l}R_{2u,1u} + B_{12}(M^2)R_{2l,1l}R_{1u,2u} + B_{11}(M^2)R_{2l,1l}R_{2u,1u}]\Gamma(-\alpha_{2l})\Gamma(-\alpha_{2u})B_b(M_b^2)\,. \tag{3.91}$$

The second and third terms in the brackets represent cuts simultaneously in s_1 and s_2 and so cannot be treated as before. The first and last terms present no new difficulty.

In the double-Regge limit it can be shown that

$$\frac{s_1 s_2}{s} = M_\perp^2 \equiv M^2 + (q_{1\perp} - q_{2\perp})^2\,, \tag{3.92}$$

where $q_{1\perp}-q_{2\perp}$ is the part of the four-momentum carried by the cluster mass M^2 transverse to the direction of p_a and p_b. In other words, the angle between $q_{1\perp}$ and $q_{2\perp}$ is fixed by $t_{1l} \approx -q_{1\perp}^2$, $t_{2l} \approx -q_{2\perp}^2$, s_1, s_2, s, and M^2. (This is not the Toller angle, but takes its place in counting variables.) One might think that the expression (3.92) could be used to remedy the problem with the propagators, since it could be used to eliminate s_1 altogether. Thus

$$R_{1,2} = \frac{1}{2}\left[\left(-\frac{s}{s_2}M_\perp^2\right)^{\alpha_1-\alpha_2} + \tau_1\tau_2\left(\frac{s}{s_2}M_\perp^2\right)^{\alpha_1-\alpha_2}\right] \times \tfrac{1}{2}[(-s)^{\alpha_2} + \tau_2 s^{\alpha_2}]\,. \tag{3.93}$$

But to be able to factor out completely the s_2 dependence of the propagator we would really like to write

$$R_{1,2} = C'\tfrac{1}{2}[(-s)^{\alpha_1-\alpha_2} + \tau_1\tau_2 s^{\alpha_1-\alpha_2}]\,\tfrac{1}{2}[(-s_2)^{\alpha_2-\alpha_1} + \tau_1\tau_2 s_2^{\alpha_2-\alpha_1}]\,\tfrac{1}{2}[(-M_\perp^2)^{\alpha_1-\alpha_2} + \tau_1\tau_2(M_\perp^2)^{\alpha_1-\alpha_2}]\,\tfrac{1}{2}[(-s)^{\alpha_2} + \tau_2 s^{\alpha_2}]\,, \tag{3.94}$$

or, combining the terms involving s,

$$R_{1,2} = C_{1,2}^{\tau_1\tau_2}\tfrac{1}{2}[(-s_2)^{\alpha_2-\alpha_1} + \tau_1\tau_2 s_2^{\alpha_2-\alpha_1}]\,\tfrac{1}{2}[(-M_\perp^2)^{\alpha_1-\alpha_2} + \tau_1\tau_2(M_\perp^2)^{\alpha_1-\alpha_2}]\,\tfrac{1}{2}[(-s)^{\alpha_1} + \tau_1 s^{\alpha_1}]\,, \tag{3.95}$$

where for positive signature $\tau_1 = \tau_2 = +$

$$C_{1,2}^{(+,+)} = \frac{\cos(\frac{1}{2}\pi\alpha_2)}{\cos(\frac{1}{2}\pi\alpha_1)\cos[\frac{1}{2}\pi(\alpha_2-\alpha_1)]}\,. \tag{3.96}$$

Of course, the replacement (3.95) is incorrect, since we mean it to represent a product of terms with fixed real axis cuts in s_2, $M_\perp^2$, and s, whereas the correct expression (3.93) has moving cuts in these variables. Therefore, in particular, (3.95) disagrees with (3.93) in phase for s, s_2, and $M_\perp^2$ away from the real axis. Nevertheless, in taking the Mellin transform we seek only the discontinuity of the integrand across cuts in s, i.e., the difference between the integrand evaluated with all integration contours aligned above right-hand cuts and below left-hand cuts and the integrand evaluated with all integration contours aligned below right-hand cuts and above left-hand cuts. Since Eq. (3.95) agrees with Eq. (3.93) when all variables approach the real axis from the *same* side, making the replacement (3.95) does not change the Mellin transform even though it changes the integrand. As a consistency check of this assertion, we have rederived the expression for the first iteration of the Reggeon-particle cut (3.85) making the replacement (3.95) for the first term of (3.79) and obtained exactly the same result. We state this result as a rule.

Rule 2. For the purposes of calculating Mellin transforms of Reggeon diagrams, the energy-plane cuts in the Reggeon propagators may be re-

arranged in any way [such as in (3.95)], provided that the rearrangement preserves the total discontinuity across all cuts.

The replacement (3.95) applied to the propagators for the upper and lower Reggeons alike then makes it possible to complete the analysis of the diagram of Fig. 19 following the techniques of the previous subsection. We find that

$$A_2^\tau(J,q_\perp)=K^\tau(J,q_\perp)\int\frac{d^2q_{1\perp}d^2q_{2\perp}}{(16\pi^3)^2}\,B_a^\tau(J-\alpha_{1u}-\alpha_{1l},q_\perp,q_{1\perp})$$
$$\times P_1^\tau(J,q_\perp,q_{1\perp})B^\tau(J,q_\perp,q_{1\perp},q_{2\perp})P_2^\tau(J,q_\perp,q_{2\perp})B_b^\tau(J-\alpha_{2u}-\alpha_{2l},q_\perp,q_{2\perp}), \tag{3.97}$$

where for $\tau_{1l}=\tau_{1u}=\tau_{2l}=\tau_{2u}=\tau=+$

$$K^{(+)}(J,q_\perp)=\frac{1}{\Gamma(-J)\cos(\frac{1}{2}\pi J)}\ ,$$

$$P_i^{(+)}(J,q_\perp,q_{i\perp})=\frac{\Gamma(-J+\alpha_{il}+\alpha_{ui})\cos[\frac{1}{2}\pi(J-\alpha_{il}-\alpha_{ui})]}{\Gamma(J-\alpha_{il}-\alpha_{ui}+1)}$$
$$\times\frac{\Gamma(-\alpha_{il})\cos(\frac{1}{2}\pi\alpha_{il})\Gamma(-\alpha_{ui})\cos(\frac{1}{2}\pi\alpha_{ui})\bar\delta_i^{J-\alpha_{il}-\alpha_{ui}+1}}{(J-\alpha_{il}-\alpha_{ui}+1)}\ ,$$

$$B^{(+)}(J,q_\perp,q_{1\perp},q_{2\perp})=\cos[\tfrac{1}{2}\pi(\alpha_{2u}-\alpha_{1u})]\cos[\tfrac{1}{2}\pi(\alpha_{2l}-\alpha_{1l})]$$
$$\times\Bigg[\frac{B_{22}^{(+)}(J-\alpha_{1l}-\alpha_{1u},q_\perp,q_{1\perp},q_{2\perp})}{\Gamma(-J+\alpha_{2u}+\alpha_{2l})\cos[\frac{1}{2}\pi(J-\alpha_{2u}-\alpha_{2l})]\cos(\frac{1}{2}\pi\alpha_{1l})\cos(\frac{1}{2}\pi\alpha_{1u})}$$
$$+\frac{B_{21}^{(\tau)}(J-\alpha_{1l}-\alpha_{2u},q_\perp,q_{1\perp},q_{2\perp})\Gamma(-J+\alpha_{1l}+\alpha_{2u})\cos[\frac{1}{2}\pi(J-\alpha_{1l}-\alpha_{2u})]}{\Gamma(-J+\alpha_{2u}+\alpha_{2l})\cos[\frac{1}{2}\pi(J-\alpha_{2u}-\alpha_{2l})]\Gamma(-J+\alpha_{1u}+\alpha_{1l})\cos[\frac{1}{2}\pi(J-\alpha_{1u}-\alpha_{1l})]}$$
$$\times\frac{1}{\cos(\frac{1}{2}\pi\alpha_{1l})\cos(\frac{1}{2}\pi\alpha_{2u})}+(1\leftrightarrow2)\Bigg]\ . \tag{3.98}$$

4. Contribution to the total cross section

It is instructive to evaluate (3.97) for the two-Pomeron cut in the forward direction and compare with what is obtained for the contribution to the total cross section of events containing two large rapidity gaps. We proceed in analogy to the discussion of the two-component model of Sec. III B 4. Since all amplitudes are even under crossing, the positive-signatured amplitudes in (3.97) can all be replaced by the modified Mellin transform (3.64). We find that the full contribution to the forward absorptive part for the diagram of Fig. 19 is

$$\mathfrak{A}_2(J,0)=\int\frac{d^2q_{1\perp}d^2q_{2\perp}}{(2\pi)^8}\,\mathfrak{B}_a(J-2\alpha_1,0,q_{1\perp})\,\frac{\bar\delta_1^{J-2\alpha_1+1}}{J-2\alpha_1+1}$$
$$\times\{\cos[\tfrac{1}{2}\pi(\alpha_1-\alpha_2)]\,\Gamma(-\alpha_1)\Gamma(-\alpha_2)\}^2\mathfrak{B}(J,0,q_{1\perp},q_{2\perp})\,\frac{\bar\delta_2^{J-2\alpha_2+1}}{J-2\alpha_2+1}\,\mathfrak{B}_b(J-2\alpha_2,0,q_{2\perp}),$$
$$\mathfrak{B}(J,0,q_{1\perp},q_{2\perp})\equiv\mathfrak{B}_{22}(J-2\alpha_2,0,q_{1\perp},q_{2\perp})(\cos\tfrac{1}{2}\pi\alpha_2)^2\,\frac{\sin(\frac{1}{2}\pi J)}{\sin[\frac{1}{2}(J-2\alpha_1)]}$$
$$+\mathfrak{B}_{21}(J-\alpha_1-\alpha_2,0,q_{1\perp},q_{2\perp})(\cos\tfrac{1}{2}\pi\alpha_1\cos\tfrac{1}{2}\pi\alpha_2)\,\frac{\sin(\frac{1}{2}\pi J)}{\sin[\frac{1}{2}\pi(J-\alpha_1-\alpha_2)]}+(1\leftrightarrow2), \tag{3.99}$$

where $\alpha_{1l}=\alpha_{1u}=\alpha_1$, $\alpha_{2l}=\alpha_{2u}=\alpha_2$, and $\bar\delta_1$ and $\bar\delta_2$ are given by (B25).

On the other hand, the differential cross section for two large gaps is obtained from the discontinuity of the integrand of (3.91) in M_a^2, M^2, and M_b^2 with all upper Reggeon propagators $R_{1u,2u}$ and $R_{2u,1u}$ complex conjugated. Thus

$$\frac{1}{2i}\,\mathrm{disc}\,A_2(s,0)_{\mathrm{gap}} = \frac{4}{(2\pi)^8}\int d^4q_1 d^4q_2\,\frac{\mathrm{disc}\,B_a(M_a^2)}{2i}\{\Gamma(-\alpha_1)\cos[\tfrac{1}{2}\pi(\alpha_1-\alpha_2)]\,\Gamma(-\alpha_2)\}^2 s_2^{2\alpha_2-2\alpha_1} s^{2\alpha_1}(M_\perp^2)^{-2\alpha_2}$$
$$\times\Big[(M_\perp^2)^{2\alpha_1}\,\frac{\mathrm{disc}\,B_{22}(M^2)}{2i}\cos^2(\tfrac{1}{2}\pi\alpha_2)$$
$$+(M_\perp^2)^{\alpha_1+\alpha_2}\exp[-i\tfrac{1}{2}\pi(\alpha_1-\alpha_2)]\,\frac{\mathrm{disc}\,B_{21}(M^2)}{2i}\cos(\tfrac{1}{2}\pi\alpha_1)\cos(\tfrac{1}{2}\pi\alpha_2)$$
$$+(M_\perp^2)^{\alpha_1+\alpha_2}\exp[i\tfrac{1}{2}\pi(\alpha_1-\alpha_2)]\,\frac{\mathrm{disc}\,B_{12}(M^2)}{2i}\cos(\tfrac{1}{2}\pi\alpha_1)\cos(\tfrac{1}{2}\pi\alpha_2)$$
$$+(M_\perp^2)^{2\alpha_2}\,\frac{\mathrm{disc}\,B_{11}(M^2)}{2i}\cos^2(\tfrac{1}{2}\pi\alpha_1)\Big] \tag{3.100}$$

is the contribution of the two-gap cross section to the absorptive part.

In the special case that the clusters are replaced by a single particle we must set

$$\begin{aligned}&\mathrm{disc}\,B_a(M_a^2,0,q_{1\perp}) = 2\pi i\,\delta(M_a^2-m_a^2)\beta_a^2(q_{1\perp}),\\ &\mathrm{disc}\,B_b(M_b^2,0,q_{2\perp}) = 2\pi i\,\delta(M_b^2-m_b^2)\beta_b^2(q_{2\perp}),\\ &(M_\perp^2)^{\alpha_i+\alpha_j}\,\mathrm{disc}\,B_{ij}(M^2,0,q_{1\perp},q_{2\perp}) = 2\pi i\,\delta(M^2-m^2)\beta_i(q_{1\perp},q_{2\perp})\beta_j^*(q_{1\perp},q_{2\perp}),\end{aligned} \tag{3.101}$$

so that

$$\frac{1}{2i}\,\mathrm{disc}\,A_2(s,0)_{\mathrm{gap}} \underset{s\to\infty}{\sim} \pi\,\frac{1}{s}\int\frac{d^2q_{1\perp}d^2q_{2\perp}}{(16\pi^3)^2}\,\frac{ds_1}{s_1}\,|T_5|^2, \tag{3.102}$$

where

$$T_5 = \beta_a(q_{1\perp})\Gamma(-\alpha_1)\Gamma(-\alpha_2)\beta_b(q_{2\perp})\{\tfrac{1}{2}[(-s_1)^{\alpha_1-\alpha_2}+s_1^{\alpha_1-\alpha_2}]\,\tfrac{1}{2}[(-s)^{\alpha_2}+s^{\alpha_2}]\beta_1(q_{1\perp},q_{2\perp})$$
$$+\tfrac{1}{2}[(-s_2)^{\alpha_2-\alpha_1}+s_2^{\alpha_2-\alpha_1}]\,\tfrac{1}{2}[(-s)^{\alpha_1}+s^{\alpha_1}]\beta_2(q_{1\perp},q_{2\perp})\} \tag{3.103}$$

is the correct expression for the 2-3 amplitude in the double-Regge limit for trajectories of positive signature.

In the general case the modified Mellin transform of the absorptive part (3.64) is

$$\mathfrak{G}_2(J,0)_{\mathrm{gap}} = \frac{1}{(2\pi)^8}\int d^2q_{1\perp}d^2q_{2\perp}\mathfrak{G}_a(J-2\alpha_1,0,q_{1\perp})\,\frac{\bar{\delta}_1^{J-2\alpha_1+1}}{J-2\alpha_1+1}\{\Gamma(-\alpha_1)\cos[\tfrac{1}{2}\pi(\alpha_1-\alpha_2)]\,\Gamma(-\alpha_2)\}^2$$
$$\times\mathfrak{G}_{\mathrm{gap}}(J,0,q_{1\perp},q_{2\perp})\,\frac{\bar{\delta}_2^{J-2\alpha_2+1}}{J-2\alpha_2+1}\,\mathfrak{G}_b(J-2\alpha_2,0,q_{2\perp}), \tag{3.104}$$

where

$$\mathfrak{G}_{\mathrm{gap}}(J,0,q_{1\perp},q_{2\perp}) \equiv \mathfrak{G}_{22}(J-2\alpha_1)\cos^2(\tfrac{1}{2}\pi\alpha_2)+\mathfrak{G}_{21}(J-\alpha_1-\alpha_2)\exp[-i\tfrac{1}{2}\pi(\alpha_1-\alpha_2)]\cos(\tfrac{1}{2}\pi\alpha_1)\cos(\tfrac{1}{2}\pi\alpha_2)+(1\leftrightarrow 2). \tag{3.105}$$

Comparing with (3.99), we see that the expressions are nearly identical with the exception that (3.99) has extra factors of $\sin(\frac{1}{2}\pi J)/\sin[\frac{1}{2}\pi(J-\alpha_i-\alpha_j)]$ and (3.105) has instead the phase $e^{-i\pi(\alpha_i-\alpha_j)/2}$. If the major part of the integral comes from $\alpha_1\simeq\alpha_2\simeq 1$, the effect of the factors is to make the sign of the full contribution to the absorptive part negative, since the cross section is obviously positive. However, for general α_1, α_2 the relative weighting of the various terms in $\mathfrak{G}(J)$ differs from $\mathfrak{G}(J)_{\mathrm{gap}}$. For this reason it is not possible to determine the full amplitude (3.99) precisely by measuring the two-gap differential cross section for various $M_a^2, M^2, M_b^2, q_{1\perp}, q_{2\perp}$.

IV. COMPARISON WITH THE TRADITIONAL REGGEON CALCULUS

In the previous section we derived the Mellin transforms of the Reggeon diagrams of Figs. 11, 13, 16, and 19 which deal with the simplest J-plane cuts formed from a particle and Reggeon and from two Reggeons. We have not extended our analysis to the general n-Reggeon cut, although such an extension is presumably straightforward but laborious with the techniques developed in Sec. III.

It is useful to compare our formulas with those of Gribov.[13] There are differences which can be

traced to the different treatment of the singularity structure of the integrand, i.e., the treatment of signature of the Reggeons, and to the more detailed treatment of the cutoff problem. Since our analysis of the singularity structure has been found to be valid in various models including the dual resonance model and models based on perturbation theory,[25] it is likely that even the diagrams studied by Gribov should be represented correctly according to our prescription.

We agree with the basic factorization property which permits the construction of a graphical theory of J-plane amplitudes. However, the correspondence between the basic J-plane amplitudes and the basic energy-plane amplitudes in our representation of the calculus differs from that of Gribov's. In the two-Reggeon graph of Fig. 13 with Mellin transform (3.59) a difference appears in the form of the integrand of (3.59) away from the pole at $J=\alpha_l+\alpha_u-1$. This difference has also been noted by Henyey and Sukhatme.[33] Because it is associated with a cutoff dependence through $\bar{\delta}$, the differences between our formula (3.59) and Gribov's can be absorbed approximately in the choice of the intercept of the bare Pomeron, which is arbitrary in the theory anyway.

In the higher-order diagram of Fig. 19 with Mellin transform (3.97) other differences appear. The cosine factors involving the trajectory parameters α_{ll} and α_{ul} are different. The "unenhanced" Gribov vertex of Fig. 20 corresponds to a fixed pole of the four-Reggeon amplitude. Because of the particular analytic structure of the four-Reggeon amplitude, a fixed pole can appear in four separate amplitudes as we see from (3.98). Thus we find that the basic vertex of Fig. 20 must have a residual J dependence which is neglected in the traditional Reggeon calculus.

These differences are probably not of much consequence for model calculations within the Reggeon field theory,[16] since the choice of vertex functions in these theories is usually made a matter of convenience, without reference to the energy-plane behavior of the scattering amplitudes. However, if one wants to maintain a consistent connection with the energy plane, then it is necessary to use the correct J-plane projection and correct treatment of signature.

V. SUMMARY OF USEFUL FORMULAS

We collect here a list of formulas useful for a phenomenology based on the iterative approach to the Pomeron advocated in Sec. I and on the results of Sec. III. It is assumed that the elastic scattering amplitude is accurately described by the two terms of lowest order in the bare-Pomeron coupling illustrated in Fig. 21. The bare Pomeron itself occurs in the shaded bubbles as a pole in the J plane.

FIG. 20. "Unenhanced vertex" in the Gribov calculus.

The contribution from the first term to the elastic amplitude (Pomeron-pole term) is the usual one:

$$A_{ab0}(s,t)\underset{s\to\infty}{\sim}-\frac{1}{2}\pi\,\frac{\beta_a^P(t)\beta_b^P(t)e^{-i\pi\alpha_P/2}s^{\alpha_P}}{\Gamma(1+\alpha_P)\sin(\frac{1}{2}\pi\alpha_P)}\,, \tag{5.1}$$

where $\alpha_P\equiv\alpha_P(t)$ is the bare-Pomeron trajectory function and $\beta_{a,b}^P(t)$ are the bare-Pomeron vertex functions. The contribution to the total cross section is given by the optical theorem

$$\sigma_{ab0}(s)\underset{s\to\infty}{\sim}\frac{1}{2}\,\pi\,\frac{\beta_a^P(0)\beta_b^P(0)s^{\alpha_P(0)-1}}{\Gamma(1+\alpha_P(0))}\,. \tag{5.2}$$

The contribution of the second term could be calculated from the J-plane projection (3.59) and (3.22) directly, which requires knowledge of the Pomeron trajectory and the partial-wave amplitudes $B_{a,b}^{\tau}(J)$. These can be determined in the forward direction ($t=0$) from inclusive experiments of the type $ac\to c+$ anything and $bd\to d+$ anything and Eq. (3.58). The elastic vertices are determined by factorization from elastic cross sections. Thus

$$\frac{\operatorname{disc}B_a(M_a^2,0,t_1,t_1)}{2\pi i}=\lim_{s\to\infty}\frac{d\sigma^{ac\to c}/dt_1dM_a^{\,2}}{[(1/16\pi)|\xi_+|^2s^{2\alpha_P-2}d\sigma_{cc}^{el}/dt_1]^{1/2}}, \tag{5.3}$$

where $\alpha_P\equiv\alpha_P(t_1)$, $\xi_+=-\pi/[2\sin(\frac{1}{2}\pi\alpha_P)\Gamma(1+\alpha_P)]$, and

$$\frac{B_a(J-2\alpha_P,0,t_1,t_1)}{\Gamma(J-2\alpha_P+1)}=\int_{M_0^2}^{\infty}dM_a^{\,2}\,\frac{\operatorname{disc}B_a(M_a^2,0,t_1,t_1)}{2\pi i}\times(M^2)^{-J-1+2\alpha_P}\,. \tag{5.4}$$

Similar expressions determine B_b. However, this procedure is awkward because it is necessary to

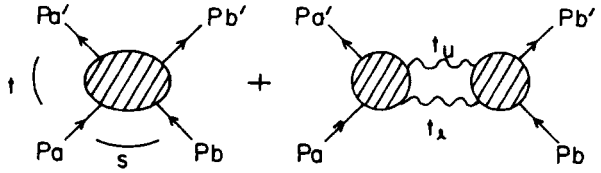

FIG. 21. Two terms of lowest order in the Pomeron coupling.

make subtractions in (5.4) to continue in J past poles, a procedure which is sensitive to a precise knowledge of the bare-Pomeron intercept and residue.

An alternative involves an approximation in (3.59) in which the J dependence of $\zeta^{(+)}$ is ignored. Thus, setting it equal to its value on the cut, we write

$$\zeta^{(+)}(J, \alpha_l, \alpha_u) \approx \sin[\tfrac{1}{2}\pi(\alpha_l + \alpha_u - 1)] \cos(\tfrac{1}{2}\pi\alpha_l) \times \cos(\tfrac{1}{2}\pi\alpha_u). \quad (5.5)$$

This has the effect of making the integrand of (3.59) proportional to that of the single gap integrand of (3.67) with a ratio independent of J. The inverse transform (3.22) can then be calculated by reversing the derivation of (3.67) which gives, in analogy to (3.66),

$$\mathrm{Im}A_{ab1}(s,t) \sim \frac{1}{8\pi^2}\int d^2q_{1\perp}\int_{M_0^2}^{s\bar{\delta}/M_b^2} dM_a^2 \int_{M_0^2}^{s\bar{\delta}/M_a^2} dM_b^2 \left[\frac{1}{2\pi i}\,\mathrm{disc}\,B_a(M_a^2, t, t_u, t_l)\right]\left[\frac{1}{2\pi i}\,\mathrm{disc}\,B_b(M_b^2, t, t_u, t_l)\right] \times \sin[\tfrac{1}{2}\pi(\alpha_l+\alpha_u-1)]\,\xi_+(\alpha_l)\xi_+(\alpha_u)s^{\alpha_l+\alpha_u-1}, \quad (5.6)$$

where $\alpha_l = \alpha_P(t_l)$, $\alpha_u = \alpha_P(t_u)$, and $\bar{\delta}$ is given by (B25). Although this expression gives only the imaginary part, it has the advantage that at $t=0$ it involves only measurable quantities and includes all "Regge contributions" to B_a and B_b. The contribution to the total cross section

$$\sigma_{ab1}(s) \sim \frac{1}{s}\,\mathrm{Im}\,A_{ab1}(s,0) \quad (5.7)$$

is therefore determined by the inclusive cross sections (5.3). Note that setting $\sin[\frac{1}{2}\pi(\alpha_l+\alpha_u-1)] \simeq -1$, which holds for $\alpha_l \simeq \alpha_u \simeq 1$, gives

$$\sigma_{ab1}(s) \approx -\sigma_{1\,\mathrm{gap}}, \quad (5.8)$$

the cross section for events with one large rapidity gap (including the elastic scattering).

The expression (5.6) includes the contribution of the J-plane cut and the poles and double poles in Fig. 21. It is sometimes interesting to isolate the contribution of the cut alone. This is given by (3.59) and (3.22):

$$A_{ab1,\mathrm{cut}}(s,t) = \int \frac{d^2q_{1\perp}}{32\pi^2} N_a^{(+)}(t, t_u, t_l) N_b^{(+)}(t, t_u, t_l)\,\xi^+(\alpha_u)\xi^+(\alpha_l)\exp[-i\tfrac{1}{2}\pi(\alpha_l+\alpha_u-1)]\,s^{\alpha_l+\alpha_u-1}, \quad (5.9)$$

which does not involve any approximations on $\zeta^{(+)}$. Since the s dependence is given explicitly, both the real and imaginary parts are known, but, of course, this is only part of the full amplitude. The fixed-pole residues at $t=0$, $t_u = t_l$ may be determined from experimental data with sum rules.[34] For example, for large L,

$$\frac{1}{2\pi i}\int_{M_0^2}^{L} dM_a^2\,\mathrm{disc}\,B_a(M_a^2, 0, t_l, t_l) = N_a^{(+)}(0, t_l, t_l) + \frac{\beta_a(0)L^{\alpha_P(0)-2\alpha_l+1}\bar{\gamma}(0, t_l, t_l)}{\alpha_P(0)-2\alpha_l+1}, \quad (5.10)$$

where it is necessary to separate the contribution of the pole term (the second term on the right) when the exponent of L is not negative. If $\bar{\gamma}$ does not vanish with the denominator in the second term, $N_a^{(+)}$ must have a compensating singularity to prevent having singularities in the physical quantities on the left. This would introduce undesirable infinities in (5.9) which, although present in the cut term by itself, are absent in the full contribution (5.6), since they are canceled by the pole and double-pole contributions. In such a case, (5.6) is more useful.

Both (5.6) and (5.1) can be used to study the various elastic differential cross sections at high energies through

$$\frac{d\sigma_{ab}}{dt} \sim \frac{|A_{ab0}(s,t) + A_{ab1}(s,t)|^2}{16\pi s^2}. \quad (5.11)$$

The expressions (5.2), (5.6), and (5.7) may be used to relate total cross sections to the inclusive experiments. In the former case it is necessary to make model assumptions about the dependence of the amplitudes away from $t=0$, $t_u = t_l$, which cannot be determined by independent experiment, and about the behavior of the real part of A_{ab1}. Some work in this direction has already met with some success,[35] although only Capella and Kaplan attempt to relate the inclusive cross section to the total cross section, and no attempts have yet been made to investigate the degree to which experiment constrains the bare intercept and coupling.

In phenomenological analyses it should be borne in mind that as with all perturbation theories,

there are no *a priori* restrictions on the choice of coupling constants and pole positions in the Reggeon calculus, although some choices may lead to more rapid convergence than others. Thus it is neither necessary that the bare-Pomeron intercept be less than or equal to 1—it could well be greater[36]—nor is it necessary that the bare-triple -Pomeron coupling vanish at zero-momentum transfer, since it is renormalized anyway.

Another potentially useful application of these results is in treating "absorptive corrections" to ordinary meson trajectory exchange in inelastic amplitudes. In this case one of the Pomerons in Fig. 21 should be replaced by a Reggeon, say α_1. For positive-signature mesons Eq. (3.59) can be adapted immediately to this application. For *negative*-signature mesons one must put $B^{\tau}_{a,b} - B^{-\tau}_{a,b}$ on the right side of (3.59) and

$$\zeta^{(+)} = \frac{-\sin(\frac{1}{2}\pi J)\cos(\frac{1}{2}\pi\alpha_u)\sin(\frac{1}{2}\pi\alpha_l)}{\cos[\frac{1}{2}\pi(J-\alpha_l-\alpha_u)]}\,,$$
$$\zeta^{(-)} = \frac{\cos(\frac{1}{2}\pi J)\cos(\frac{1}{2}\pi\alpha_u)\sin(\frac{1}{2}\pi\alpha_l)}{\sin[\frac{1}{2}\pi(J-\alpha_l-\alpha_u)]}\,. \tag{5.12}$$

The cut appears in the negative-signatured amplitude in this case.

ACKNOWLEDGMENT

The author is greatly indebted to C. Edward Jones and Francis Low, who collaborated in the early stages of this work.

APPENDIX A: ANALYSIS OF A SIMPLE CUT DIAGRAM BASED ON THE DUAL RESONANCE MODEL

We sketch here an alternative method to obtaining the Mellin transform of Reggeon diagrams, which is based on knowledge of the multiple Mellin transform of the loop integrand. This also provides an alternative justification for the method used in Sec. III of dropping terms lacking singularities in the cluster masses.

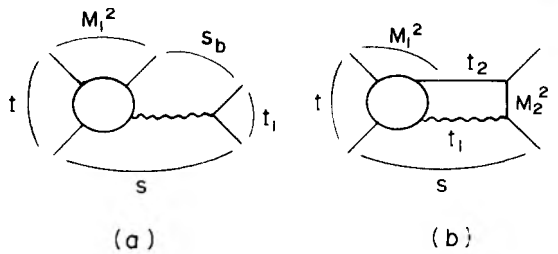

FIG. 22. Amplitude with a J-plane cut (b) constructed from the five-point function (a).

In the dual resonance model the five-point function B_5 of Fig. 22(a) has the helicity asymptotic behavior[25]

$$B_5 \underset{\substack{s\to\infty \\ t,\, M_1^2,\, s_b,\, t_1 \text{ fixed}}}{\sim} (-s)^{\alpha_0(t)} f(s_b, t, t_1) + (-s)^{\alpha_1(t)} g(M_1^2, t, t_1), \tag{A1}$$

where $\alpha_0(t)$ and $\alpha_1(t_1)$ are leading trajectories in the t and t_1 channels. The B_5 amplitude can be used to construct a four-particle amplitude $A(s,t)$ with a J-plane cut by inserting extra propagators M_2^2 and t_2 as shown in Fig. 22(b) so that

$$A(s,t) = \frac{-i}{(2\pi)^4}\int_D d^4q_1\, B_5(t, M_1^2, s, t_1, s_b = m^2) \times \frac{1}{M_2^2 - m^2}\,\frac{1}{t_2 - m^2}\,, \tag{A2}$$

where $q_1^2 = t_1$. We have argued in Sec. III that for the purposes of calculating the Mellin transform of $A(s,t)$ the first term in (A1) may be ignored. We show in what way this is true for this simple example, in which the Mellin transform can be evaluated directly.

We first write the multiple Mellin representation of the five-point function[25]:

$$B_5 \sim \frac{1}{(2\pi i)^3}\int dJ_0\, dJ_1\, d\lambda\, \Gamma(-J_0+\lambda)\Gamma(-J_1+\lambda)\Gamma(-\lambda)(-M_1^2)^{J_0-\lambda}(-s_b)^{J_1-\lambda}(-s)^{\lambda}\beta(J_0, J_1, \lambda; t, t_1)\,, \tag{A3}$$

where β has poles at $J_0 = \alpha_0(t)$ and $J_1 = \alpha_1(t_1)$ but no poles in λ and the contours are drawn initially to the right of these poles and to the left of the poles in the Γ functions. The helicity asymptotic behavior (A1) follows directly from this representation, if the λ contour is shifted to the left. The first term arises because of the pole at $\lambda = \alpha_0(t)$ due to a pinch of the J_0 contour between poles in $\Gamma(-J_0+\lambda)$ and the pole at $J_0 = \alpha_0(t)$. The second term arises because of a corresponding pinch of the J_1 contour. Thus we see that the presence of the first term in (A1) is directly attributable to the Regge pole at $J_0 = \alpha_0(t)$.

We shall now use (A3) in (A2) and perform the Mellin transform of $A(s,t)$ directly. We use the Sudakov variable approximations on the loop integration outlined in Sec. III. Therefore, we write

$$\int d^4q_1 \to \tfrac{1}{2}|s|\int d^2q_\perp\, d\alpha\, d\beta \tag{A4}$$

and

$$A(s,t)=\frac{1}{(2\pi i)^3}\int d^2q_\perp\int dJ_0\,dJ_1\,d\lambda\,\Gamma(-J_0+\lambda)\Gamma(-J_1+\lambda)\Gamma(-\lambda)(-m^2)^{J_1-\lambda}(-s)^\lambda\,\frac{\beta(J_1,J_2,\lambda;t,t_1)}{t_2-m^2}\,I(s,t,q_\perp)\,, \tag{A5}$$

where

$$I(s,t,q_\perp)=\frac{-i}{(2\pi)^4}\int_D \tfrac{1}{2}|s|\,d\alpha\,d\beta(-M_1^2)^{J_0-\lambda}\,\frac{1}{M_2^2-m^2}\,. \tag{A6}$$

To evaluate $I(s,t,q_\perp)$ we first take its discontinuity across its right-hand cuts in s, according to the procedures of Sec. III. Thus from (3.36)

$$\mathrm{disc}_s I(s,t,q_\perp)=\frac{1}{(2\pi)^3}\,\frac{1}{2s}\int_0^{\bar\delta s/M_0^2}dM_1^2\left[-2i\sin\pi(J_0-\lambda)(M_1^2)^{J_0-\lambda}\right]\int_0^{\bar\delta s/M_1^2}dM_2^2\,\delta(M_2^2-m^2)\,, \tag{A7a}$$

$$\mathrm{disc}_s I(s,t,q_\perp)=\frac{1}{16\pi^3 s}\,\frac{\left[-2i\sin\pi(J_0-\lambda)\bar\delta^{J_0-\lambda+1}s^{J_0-\lambda+1}\right]}{J_0-\lambda+1}\,, \tag{A7b}$$

provided $\mathrm{Re}(J_0-\lambda+1)>0$, which is easily arranged in the initial placement of the contour. For other values of J_0, λ we use (A7b) as the correct analytic continuation. Since I has only right-hand cuts and no fixed powers it follows that

$$I(s)=\frac{1}{16\pi^3}\,\frac{(-s)^{J_0-\lambda}\bar\delta^{J_0-\lambda+1}}{J_0-\lambda+1}\,. \tag{A8}$$

When this is inserted into (A5), the Mellin transform of $A(s,t)$ can be read off immediately:

$$A(s,t)=\frac{1}{2\pi i}\int dJ_0\Gamma(-J_0)(-s)^{J_0}\int d^2q_{1\perp}\int\frac{dJ_1d\lambda}{(2\pi i)^2}\,\frac{\Gamma(-J_0+\lambda)\Gamma(-J_1+\lambda)\Gamma(-\lambda)}{\Gamma(-J_0)}\,\frac{1}{16\pi^3}\,\frac{(-m^2)^{J_1-\lambda}}{J_0-\lambda+1}$$
$$\times\,\frac{\beta(J_0,J_1,\lambda;t,t_1)}{t_2-m^2}\,\bar\delta^{J_0-\lambda+1}\,, \tag{A9}$$

so that

$$A^\tau(J,t)=\frac{1}{16\pi^3}\int d^2q_{1\perp}\int\frac{dJ_1d\lambda}{(2\pi i)^2}\,\frac{\Gamma(-J+\lambda)\Gamma(-J_1+\lambda)\Gamma(-\lambda)}{\Gamma(-J)(J-\lambda+1)}(-m^2)^{J_1-\lambda}\bar\delta^{J-\lambda+1}\,\frac{\beta(J,J_1,\lambda;t,t_1)}{t_2-m^2}\,. \tag{A10}$$

Because there is no integration over J in (A10) there is no longer a singularity at $\lambda=\alpha_0(t)$ in the λ plane. The singularity at $\lambda=\alpha_1(t)$ remains, however, and $A(J,t)$ inherits the singularity of β at $J=\alpha_0(t)$. This is the significance of dropping the first term in (A1) in Sec. III. The expression (A10) actually contains the whole spectrum of cuts due to the poles and daughters at $J_1=\alpha_1(t)$, $\alpha_1(t)-1$, etc. Since the cutoff prescription makes the daughter poles less important, we keep only the first term:

$$A^\tau(J,t)=\frac{1}{16\pi^3}\int d^2q_{1\perp}\,\frac{\Gamma(-J+\alpha_1)\Gamma(-\alpha_1)}{\Gamma(-J)(J-\alpha_1+1)}\,\bar\delta^{J-\alpha_1+1}$$
$$\times\,\frac{b(J,t,t_1)}{t_2-m^2}\,, \tag{A11}$$

where

$$b(J,t,t_1)=\left[\mathrm{Res}_{J=\alpha_1}\beta(J,J_1,\lambda;t,t_1)\right]\Big|_{\lambda=\alpha_1}\,. \tag{A12}$$

This expression is to be compared with (3.50), with which it agrees at least to the extent that the amplitude in Fig. 22(b) has only a pole in M_2^2 and the Regge trajectories α_0 and α_1 are exchange-degenerate in this simple example.

The results of this Appendix and that of Sec. III were obtained using two different approaches. Here we used the full loop integrand with its singularity structure expressed through a multiple Mellin transform. In Sec. III we dispensed with the Mellin transform of the loop integrand, but dropped those terms in the integrand which lacked singularities in M^2, since they did not contribute to the Mellin transform of the integral. The results are the same, nevertheless.

The approach presented here is more like that used in the rigorous analysis of the cut problem,[11] since it deals directly with the J-plane representation of the loop integrand. However, this approach becomes rapidly more cumbersome when it is applied to the most general Reggeon diagram and so we chose the more direct method presented in Sec. III.

APPENDIX B: SINGULARITIES OF THE BOX GRAPH WITH FIXED INTERNAL MOMENTUM TRANSFER ANALYZED IN TERMS OF ANGULAR VARIABLES

In the text we need to evaluate singularities in s of the box graph when the integration over the loop momentum is interrupted so that two internal momentum transfers are fixed at an arbitrary value. Consider the graph of Fig. 23 and define the variables

$$\begin{aligned}
&q_0 = q_1 + q_2 ,\\
&t = q_0^2 ,\ t_1 = q_1^2 ,\ t_2 = q_2^2 ,\\
&k_a = p_a - q_1 ,\ k_b = p_b + q_1 ,\\
&k_a^2 = M_a^2 ,\ k_b^2 = M_b^2 ,\\
&p_a^2 = (p_a')^2 = p_b^2 = (p_b')^2 = m^2 ,\\
&s = (p_a + p_b)^2 ,\\
&u = (p_a' - p_b)^2 = -t - s + 4m^2 ,\\
&u_b = (p_b + q_2)^2\\
&\quad = t_1 + t_2 + 2m^2 - t - M_b^2 .
\end{aligned} \tag{B1}$$

We want to evaluate discontinuities across cuts in s in the integral

$$A(s,t) = \int d^4q_1 B_a(M_a^2, t_1, t_2) B_b(M_b^2, t_1, t_2) \times \delta(t_1 - q_1^2)\delta(t_2 - q_2^2) \tag{B2}$$

in two cases:

$$\begin{aligned}
&\textit{Case I}\quad B_a = \frac{1}{M_a^2 - M^2 + i\epsilon} ,\ B_b = \frac{1}{M_b^2 - M^2 + i\epsilon} ,\\
&\textit{Case II}\quad B_a = \frac{1}{M_a^2 - M^2 + i\epsilon} ,\ B_b = \frac{1}{u_b - M^2 + i\epsilon} ,
\end{aligned} \tag{B3}$$

i.e., poles in M_a^2 and M_b^2 on the right in B_a and B_b and a pole in M_a^2 on the right and in M_b^2 on the left. We shall do this for $t<0$, but for arbitrary choice of t_1 and t_2. We shall choose a parameterization for the q_1 integration which requires that we separate these cases in turn into two, according to the sign of

$$\lambda(t, t_1, t_2) = t^2 + t_1^2 + t_2^2 - 2t_1t_2 - 2tt_1 - 2tt_2 . \tag{B4}$$

We construct the momenta in a particular Lorentz frame so that,

Case A: $\lambda < 0$.

$$\begin{aligned}
&p_a = (p, 0, 0, \tfrac{1}{2}\sqrt{-t}) ,\\
&p_a' = (p, 0, 0, -\tfrac{1}{2}\sqrt{-t}) ,\\
&q_0 = (0, 0, 0, \sqrt{-t}),
\end{aligned}$$

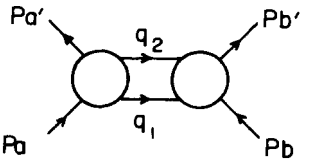

FIG. 23. Notation for box graph.

$$\begin{aligned}
q_1 &= (-q\sinh\theta_1, -q\cosh\theta_1\cos\phi ,\\
&\quad -q\cosh\theta_1\sin\phi, (t_2 - t_1 - t)/2\sqrt{-t}) ,\\
q_2 &= (q\sinh\theta_1, q\cosh\theta_1\cos\phi, q\cosh\theta_1\sin\phi ,\\
&\quad (t_1 - t_2 - t)/2\sqrt{-t}) ,\\
p_b &= (p\cosh\theta, p\sinh\theta, 0, -\tfrac{1}{2}\sqrt{-t}) ,\\
p_b' &= (p\cosh\theta, p\sinh\theta, 0, \tfrac{1}{2}\sqrt{-t}) ,\\
p &= (m^2 - \tfrac{1}{4}t)^{1/2} ,\quad q = (-\lambda)^{1/2}/2\sqrt{-t} .
\end{aligned} \tag{B5}$$

[We use the notation $p = (p_0, p_1, p_2, p_3)$ and metric $g_{00} = 1$, $g_{ii} = -1$.]

The integral then becomes

$$\int d^4q_1 = \int dt_1\, dt_2 \tfrac{1}{2}\sqrt{-\lambda} \int_{-\infty}^{\infty} d\sinh\theta_1 \int_0^{2\pi} d\phi \tag{B6}$$

and the invariants are

$$\begin{aligned}
&s = 2p^2(1 + \cosh\theta) ,\\
&M_a^2 = m^2 + \tfrac{1}{2}(t_1 + t_2 - t) + 2pq\sinh\theta_1 ,\\
&M_b^2 = m^2 + \tfrac{1}{2}(t_1 + t_2 - t) + 2pq\sinh\theta_2 ,\\
&\sinh\theta_2 \equiv \sinh\theta\cosh\theta_1\cos\phi - \sinh\theta_1\cosh\theta .
\end{aligned} \tag{B7}$$

Case B: $\lambda < 0$.

$$\begin{aligned}
p_a &= (p, 0, 0, \tfrac{1}{2}\sqrt{-t}) ,\\
p_a' &= (p, 0, 0, -\tfrac{1}{2}\sqrt{-t}) ,\\
q_1 &= (-q\cosh\theta_1, -q\sinh\theta_1\cos\phi ,\\
&\quad -q\sinh\theta_1\sin\phi, (t_2 - t_1 - t)/2\sqrt{-t}) ,\\
q_2 &= (q\cosh\theta_1, q\sinh\theta_1\cos\phi, q\sinh\theta_1\sin\phi ,\\
&\quad (t_1 - t_2 - t)/2\sqrt{-t}) ,\\
p_b &= (p\cosh\theta, p\sinh\theta, 0, -\tfrac{1}{2}\sqrt{-t}) ,\\
p_b' &= (p\cosh\theta, p\sinh\theta, 0, \tfrac{1}{2}\sqrt{-t}) ,\\
p &= (m^2 - \tfrac{1}{4}t)^{1/2} ,\quad q = \lambda^{1/2}/2\sqrt{-t} .
\end{aligned} \tag{B8}$$

The integral then becomes

$$\int d^4q_1 = \int dt_1\, dt_2 \tfrac{1}{2}\sqrt{\lambda} \left(\int_{-\infty}^{1} + \int_{1}^{\infty} \right) d\cosh\theta_1 \int_0^{2\pi} d\phi . \tag{B9}$$

The invariants are

$$
\begin{aligned}
&s = 2p^2(1+\cosh\theta)\,,\\
&M_a{}^2 = m^2 + \tfrac{1}{2}(t_1+t_2-t) + 2pq\cosh\theta_1\,,\\
&M_b{}^2 = m^2 + \tfrac{1}{2}(t_1+t_2-t) + 2pq\cosh\theta_2\,,\\
&-\cosh\theta_2 \equiv \cosh\theta\cosh\theta_1 - \sinh\theta\sinh\theta_1\cos\phi\,.
\end{aligned}
\tag{B10}
$$

The case $\lambda<0$ is the region of interest in evaluating the s- and u-channel discontinuities. We shall see that the $\lambda>0$ region does not produce singularities adjacent to the s-channel physical region. We consider the various cases in order:

Case A, $\lambda<0$, *Case I*. We are interested in the singularities of the following integral as a function of s, or equivalently $\cosh\theta$:

$$
\begin{aligned}
A(s,t) &= \int_{\lambda<0} d^4q_1 \frac{\delta(t_1-q_1{}^2)\delta(t_2-q_2{}^2)}{(M_a{}^2-M^2+i\epsilon)(M_b{}^2-M^2+i\epsilon)}\\
&= \int \frac{1}{2}\frac{\sqrt{-\lambda}\,d\sinh\theta_1 d\phi}{(2pq)^2(\sinh\theta_1-\sinh\theta_{1R})(\sinh\theta_2-\sinh\theta_{2R})}\,,
\end{aligned}
\tag{B11}
$$

where $\sinh\theta_{1R}$ and $\sinh\theta_{2R}$ are the values of $\sinh\theta_1$ and $\sinh\theta_2$ when $M_a{}^2$ and $M_b{}^2$ are at the respective pole positions. From (B7) we see that as ϕ ranges from 0 to 2π, θ_2 ranges from $-\theta-\theta_1$ to $\theta-\theta_1$. Therefore if we make the change of variables

$$
\begin{aligned}
d\phi &= \frac{d\sinh\theta_2}{\sinh\theta\cosh\theta_1\sin\phi}\\
&= \frac{d\sinh\theta_2}{\sqrt{K}}\,,\\
K &= -1-\sinh^2\theta_2-\sinh^2\theta_1+\cosh^2\theta\\
&\quad -2\sinh\theta_2\sinh\theta_1\cosh\theta\,,
\end{aligned}
$$

the position of the $\sinh\theta_2$ contour is as shown in Fig. 24. The contour runs between two branch points corresponding to the vanishing of $\sin\phi$. When either end point collides with the pole at θ_{2R} the integral becomes singular as a function of θ_1. These singularities appear at

$$
\begin{aligned}
&\theta_1 = \theta-\theta_{2R}\,,\\
&\theta_1 = -\theta-\theta_{2R}\,,
\end{aligned}
\tag{B12}
$$

as shown in Fig. 25. The contour of integration lies initially on the real axis, and we have drawn a branch cut between the two singularities introduced by the integration over ϕ_1.

The $\sinh\theta_1$ contour is trapped when the branch points collide with the pole at $\sinh\theta_{1R}$. This produces a singularity in θ and therefore in s at

$$
\theta = \theta_{1R}+\theta_{2R}\,,
\tag{B13}
$$

or in terms of s

$$
\begin{aligned}
\lambda(s-4M^2) &= (t_1-t_2)^2 4(m^2-M^2) - 4t_1t_2t\\
&\quad +4(M^2-m^2)(t_1+t_2)t + t\,4(M^2-m^2)^2\,.
\end{aligned}
\tag{B14}
$$

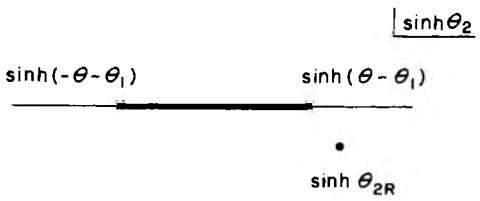

FIG. 24. Position of contour and pole in $\sinh\theta_2$.

This does not correspond to the usual normal threshold $s=4M^2$ of the box graph since the integration over t_1 and t_2 has not been carried out. It is rather like an extension of an $s-t$ double-spectral function but into an unphysical region with $t<0$ and $\lambda<0$. The actual singularity of the box graph may be recovered by considering the integration over t_1 and t_2 with $\lambda<0$. In this case the actual singularities in s appear at the extrema of $s(t_1,t_2)$ given by (B14) with respect to variation in t_1 and t_2 when $\lambda<0$. These extrema occur at two points

$$
\begin{aligned}
&t_1 = t_2 = m^2-M^2\,, \quad s=4M^2\\
&t_1 = t_2 = \tfrac{1}{2}t+M^2-m^2\,, \quad u=0
\end{aligned}
\tag{B15}
$$

as illustrated in the Mandelstam plot of Fig. 26. Since our parameterization is invalid immediately outside the s-channel physical region (the upper pie slice in Fig. 26), we cannot discuss the extension of the cut outside, but naturally we do not anticipate any difficulties. Clearly, the branch cut in θ at $\theta_{1R}+\theta_{2R}$ is associated with the normal threshold singularity at $s=4M^2$.

Case A, $\lambda<0$, *Case II*. In this case the singularity in $\sinh\theta_2$ appears at

$$
\begin{aligned}
u_b - M^2 + i\epsilon &= t_1+t_2+2m^2-t-M^2\\
&= m^2+\tfrac{1}{2}(t_1+t_2-t)+2pq\sinh\theta_{2L}\,.
\end{aligned}
\tag{B16}
$$

The $i\epsilon$ prescription for θ_{2L} is opposite that of θ_{2R} in the previous case. Therefore, the singularity in θ_1 at $\theta-\theta_{2L}$ and $-\theta-\theta_{2R}$ is in the lower half plane and cannot trap the contour. Thus a combination of left-hand and right-hand singularities in $M_a{}^2$ and $M_b{}^2$ cannot produce a singularity in the s-channel physical region. Of course, in the u-channel physical region we could reparameterize

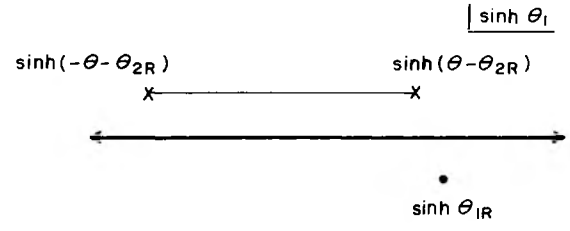

FIG. 25. Position of branch cut and pole in $\sinh\theta_1$

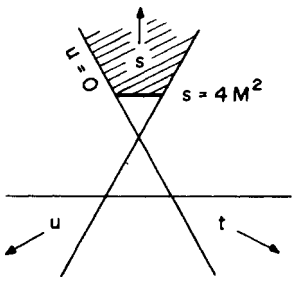

FIG. 26. Shaded region indicates location of discontinuity in s at fixed t.

the four-momenta and discover that Cases I and II interchange roles. Therefore, the combination of of two right-hand or two left-hand singularities generates physical s-channel singularities and a combination of right and left generates physical u-channel singularities.

Case B, $\lambda > 0$, *Case I*. We want to locate the singularities of the following integral as a function of s:

$$A(s,t) = \int_{\lambda>0} d^4q_1 \frac{1}{(M_a^2 - M^2 + i\epsilon)} \frac{1}{(M_b^2 - M^2 + i\epsilon)} \times \delta(t_1 - q_1^2)\delta(t_2 - q_2^2), \tag{B17}$$

where

$$M^2 - i\epsilon = m^2 + \tfrac{1}{2}(t_1 + t_2 - t) + 2pq\cosh\theta_{1R}$$

and $\theta_{1R} = \theta_{2R}$ are the locations of the pole singularities in θ_1 and θ_2 as defined in (B8)–(B10). Let the integral be expressed in terms of the parameters of (B9). As ϕ varies throughout its range, $\cosh\theta_2$ takes on the following values:

$$\cosh\theta_2 \in \begin{cases} [-\cosh(\theta_1+\theta), -\cosh(\theta-\theta_1)] \text{ for } \cosh\theta_1 > 1, \\ [\cosh(\theta_1-\theta), \cosh(\theta_1+\theta)] \text{ for } \cosh\theta_1 < -1. \end{cases} \tag{B18}$$

Now if

$$\cosh\theta_{2R} = \cosh\theta_{1R} > 1 \tag{B19}$$

the collisions $\cosh\theta_{2R} = \cosh(\theta_1 \pm \theta)$ generate singularities adjacent to the $\cosh\theta_1 < -1$ contour when s is in the physical region. Therefore, no pinching can occur with the pole at $\cosh\theta_1 = \cosh\theta_{1R} > 1$. When $\cosh\theta_{2R} = \cosh\theta_{1R} < -1$, the singularities produced by the ϕ integration once again lie adjacent to the opposite part of the $\cosh\theta_1$ contour from the pole and cannot pinch. Hence no physical region singularities in s arise from this integral.

Case B, $\lambda > 0$, *Case II*. We have the following:

$$A(s,t) = \int_{\lambda>0} d^4q_1 \frac{1}{M_a^2 - M^2 + i\epsilon} \frac{1}{u_b - M^2 + i\epsilon} \times \delta(t_1 - q_1^2)\delta(t_2 - q_2^2), \tag{B20}$$

$$M^2 - i\epsilon = m^2 + \tfrac{1}{2}(t_1 + t_2 - t) + 2pq\cosh\theta_{1R},$$

$$t_1 + t_2 - t + 2m^2 - M^2 + i\epsilon = m^2 + \tfrac{1}{2}(t_1 + t_2 - t) + 2pq\cosh\theta_{2L},$$

$$\cosh\theta_{1R} = -\cosh\theta_{2L}.$$

The range of $\cosh\theta_2$ is still given by (B18), but unlike the previous example singularities are generated in s. If $\cosh\theta_{2L} < -1$, then the ϕ integration produces branch-point singularities in $\cosh\theta_1$ at $\cosh(\theta_1 \pm \theta) = -\cosh\theta_{2L}$. The location of the branch points depends on whether θ is larger or smaller than θ_{2L} as shown in Fig. 27. Only when $\theta > \theta_{2L}$ can a pinch occur and this happens at

$$\theta = \theta_{1R} + \theta_{2L} \tag{B21}$$

or

$$\lambda s = -4t[M^2 - m^2 - \tfrac{1}{2}(t_1 + t_2 - t)]^2.$$

In order to interpret this singularity in terms of the well-known singularities of the box diagram, it is necessary to consider the integration over t_1 and t_2. The actual singularity in s in the box appears at the extrema of $s(t_1, t_2)$ with respect to variations in t_1 and t_2 subject to the constraints of our parameterization. The extrema of (B21) occur at

$$t_1 = t_2 = \tau = -m^2 + M^2 + \tfrac{1}{2}t \text{ and } s = 0,$$

$$t_1 = t_2 = \tau = m^2 - M^2 \text{ and } u = 4M^2$$

However, since both of these points lie outside the s-channel physical region we conclude that no sin-

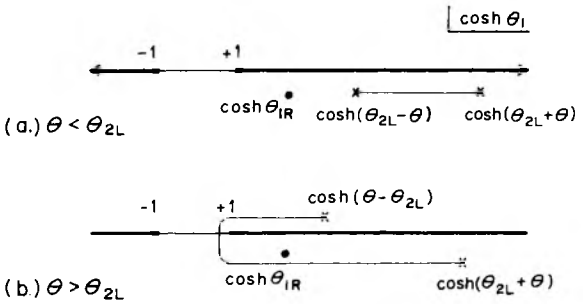

FIG. 27. Location of branch cut and contour in $\cosh\theta_1$.

gularity adjacent to the s-channel physical region can be produced by this pinch.

There are also various end-point singularities, for example when $\cosh\theta_{1R}=1$, but it can be shown that these also do not correspond to singularities adjacent to the s-channel physical region.

We conclude from this analysis that in taking the discontinuity across s-channel and u-channel cuts we need consider only the region $\lambda<0$ in the integration over t_1 and t_2 and that the usual combinations of right- and left-hand singularities in $M_a{}^2$ and $M_b{}^2$ contribute to the right- and left-hand cuts in s.

In terms of Sudakov variables in the approximation that

$$t_1\approx-(\vec{q}_{1\perp})^2\,,\quad t\approx(-\vec{q}_\perp)^2$$
$$t_2\approx-(\vec{q}_{1\perp}-\vec{q}_\perp)^2 \tag{B22}$$

the region $\lambda<0$ is simply the whole real $\vec{q}_{1\perp}$ plane.

Since at fixed t_1 and t_2 the physical discontinuity in Case A exists only for

$$\theta>\theta_{1R}+\theta_{2L}\,,\quad \lambda<0\,, \tag{B23}$$

we see from (B7) that at large θ and large θ_{1R} and θ_{2L} the range of $M_a{}^2$ and $M_b{}^2$ is restricted so that

$$q^2 s\geq M_a{}^2 M_b{}^2$$

or (B24)

$$\frac{(-\lambda)}{-4t}\,s\geq M_a{}^2 M_b{}^2\,.$$

Thus the cutoff in the text should be replaced by the smaller of the kinematical cutoff and that required in the text to establish Pomeron exchange

$$\bar{\delta}=\min[\,\delta,\,-\lambda/(-4t)] \tag{B25}$$

in order to satisfy this kinematical constraint, which does not arise in our approximate Sudakov variable analysis.[28,31]

APPENDIX C: PRODUCT RULE FOR MELLIN TRANSFORMS

Suppose we are given that $g(s)$ is real analytic with Mellin transform

$$g(s)\underset{s\to\infty}{\sim}\frac{-1}{2\pi i}\int_C dJ\;\Gamma(-J)\sum_\tau g^\tau(J)\tfrac{1}{2}[(-s)^J+\tau s^J]\,, \tag{C1}$$

and we seek the Mellin transform of

$$f(s)=g(s)\tfrac{1}{2}[(-s)^\alpha+\sigma s^\alpha]\,. \tag{C2}$$

It suffices to construct an expression which has the same discontinuity across right- and left-hand cuts in s. If we write $s=|s|e^{i\theta}$, then for $0<\theta<\pi$,

$$(-s)^J+s^J=[\,2e^{-i\pi J/2}\cos(\tfrac{1}{2}\pi J)]\,|s|^J e^{i\theta J}\,,$$
$$(-s)^J-s^J=[\,-2ie^{-i\pi J/2}\sin(\tfrac{1}{2}\pi J)]\,|s|^J e^{i\theta J}\,. \tag{C3}$$

For $\theta\to-\theta$ the expression on the right is the complex conjugate. Therefore, it can be shown that

$$\tfrac{1}{2}[(-s)^J+s^J]\,\tfrac{1}{2}[(-s)^\alpha+s^\alpha]$$
$$=\frac{\cos(\frac{1}{2}\pi J)\cos(\frac{1}{2}\pi\alpha)}{\cos[\,\frac{1}{2}\pi(J+\alpha)]}\,\tfrac{1}{2}[(-s)^{J+\alpha}+s^{J+\alpha}]\,,$$
$$\tfrac{1}{2}[(-s)^J-s^J]\,\tfrac{1}{2}[(-s)^\alpha+s^\alpha] \tag{C4}$$
$$=\frac{\sin(\frac{1}{2}\pi J)\cos(\frac{1}{2}\pi\alpha)}{\sin[\,\frac{1}{2}\pi(J+\alpha)]}\,\tfrac{1}{2}[(-s)^{J+\alpha}-s^{J+\alpha}]$$

for the entire complex plane excluding the real axis. Inserting these expressions into the equation for $f(s)$ obtained from (C1) and (C2) we find that for $\sigma=+$

$$f(s)\underset{s\to\infty}{\sim}-\frac{1}{2\pi i}\int_C dJ\;\Gamma(-J)\Big\{g^+(J)\,\frac{\cos(\frac{1}{2}\pi J)\cos(\frac{1}{2}\pi\alpha)}{\cos[\,\frac{1}{2}\pi(J+\alpha)]}\,\tfrac{1}{2}[(-s)^{J+\alpha}+s^{J+\alpha}]$$
$$+g^-(J)\,\frac{\sin(\frac{1}{2}\pi J)\cos(\frac{1}{2}\pi\alpha)}{\sin[\,\frac{1}{2}\pi(J+\alpha)]}\,\tfrac{1}{2}[(-s)^{J+\alpha}-s^{J+\alpha}]\Big\}\,. \tag{C5}$$

Changing variables $J+\alpha\to J$, we obtain

$$f^\tau(J)=\bar{C}^\tau(J,\alpha)g^\tau(J-\alpha)\,,$$

$$\bar{C}^{(+)}(J,\alpha)=\frac{\Gamma(-J+\alpha)}{\Gamma(-J)}\,\frac{\cos[\,\frac{1}{2}\pi(J-\alpha)]\cos(\frac{1}{2}\pi\alpha)}{\cos(\frac{1}{2}\pi J)}\,,$$

$$\bar{C}^{(-)}(J,\alpha)=\frac{\Gamma(-J+\alpha)}{\Gamma(-J)}\,\frac{\sin[\,\frac{1}{2}\pi(J-\alpha)]\cos(\frac{1}{2}\pi\alpha)}{\sin(\frac{1}{2}\pi J)} \tag{C6}$$

for $\sigma=+$. Similarly, it can be shown that for $\sigma=-$

$$f^\tau(J)=\bar{C}^\tau_{(-)}(J,\alpha)g^{-\tau}(J-\alpha)\,,$$

$$\bar{C}^{(+)}_{(-)}(J,\alpha)=\frac{\Gamma(-J+\alpha)}{\Gamma(-J)}\,\frac{\{-\sin[\,\frac{1}{2}\pi(J-\alpha)]\sin(\frac{1}{2}\pi\alpha)\}}{\cos(\frac{1}{2}\pi J)}\,,$$
$$\bar{C}^{(-)}_{(-)}(J,\alpha)=\frac{\Gamma(-J+\alpha)}{\Gamma(-J)}\,\frac{\cos[\,\frac{1}{2}\pi(J-\alpha)]\sin(\frac{1}{2}\pi\alpha)}{\sin(\frac{1}{2}\pi J)}\,. \tag{C7}$$

If

$$h(s)=\tfrac{1}{2}[(-s)^{\alpha_1}+s^{\alpha_1}]\,\tfrac{1}{2}[(-s)^{\alpha_2}+s^{\alpha_2}]f(s)$$

then by the same token

$$h^{\tau}(J) = C^{\tau}(J, \alpha_l, \alpha_u) g^{\tau}(J - \alpha_l - \alpha_u),$$

$$C^{(+)}(J, \alpha_l, \alpha_u) = \frac{\Gamma(-J + \alpha_l + \alpha_u)}{\Gamma(-J)} \frac{\cos[\frac{1}{2}\pi(J - \alpha_l - \alpha_u)] \cos(\frac{1}{2}\pi\alpha_l) \cos(\frac{1}{2}\pi\alpha_u)}{\cos(\frac{1}{2}\pi J)},$$

$$C^{(-)}(J, \alpha_l, \alpha_u) = \frac{\Gamma(-J + \alpha_l + \alpha_u)}{\Gamma(-J)} \frac{\sin[\frac{1}{2}\pi(J - \alpha_l - \alpha_u)] \cos(\frac{1}{2}\pi\alpha_l) \cos(\frac{1}{2}\pi\alpha_u)}{\sin(\frac{1}{2}\pi J)}. \quad \text{(C8)}$$

If

$$h(s) = \tfrac{1}{2}[(-s)^{\alpha_l} - s^{\alpha_l}] \tfrac{1}{2}[(-s)^{\alpha_u} + s^{\alpha_u}] f(s), \quad \text{(C9)}$$

then

$$h^{\tau}(J) = C^{\tau}_{(-)}(J, \alpha_l, \alpha_u) g^{-\tau}(J - \alpha_l - \alpha_u), \quad \text{(C10)}$$

where

$$C^{(+)}_{(-)}(J, \alpha_l, \alpha_u) = \frac{\Gamma(-J + \alpha_l + \alpha_u)}{\Gamma(-J)} \frac{\{-\sin[\frac{1}{2}\pi(J - \alpha_l - \alpha_u)] \sin(\frac{1}{2}\pi\alpha_l) \cos(\frac{1}{2}\pi\alpha_u)\}}{\cos(\frac{1}{2}\pi J)},$$

$$C^{(-)}_{(-)}(J, \alpha_l, \alpha_u) = \frac{\Gamma(-J + \alpha_l + \alpha_u)}{\Gamma(-J)} \frac{\cos[\frac{1}{2}\pi(J - \alpha_l - \alpha_u)] \sin(\frac{1}{2}\pi\alpha_l) \cos(\frac{1}{2}\pi\alpha_u)}{\sin(\frac{1}{2}\pi J)}. \quad \text{(C11)}$$

---

*Work supported in part through funds provided by the U. S. Atomic Energy Commission under Contract No. AT(11-1)-3069.

†On leave until July, 1975 at Theory Division, CERN, Geneva, Switzerland.

[1]I. Ya. Pomeranchuk, Zh. Eksp. Teor. Fiz. 30, 423 (1956) [Sov. Phys.—JETP 3, 306 (1956)]; I. Ya. Pomeranchuk and L. B. Okun, *ibid.* 30, 424 (1956) [*ibid.* 3, 307 (1956)]; I. Ya. Pomeranchuk, *ibid.* 34, 725 (1958) [*ibid.* 7, 499 (1958)]; G. F. Chew and S. C. Frautschi, Phys. Rev. Lett. 8, 41 (1962).

[2]M. Jacob, CERN Report No. TH. 1683-CERN, 1973 (unpublished), based on data in the region $0.01 < |t| < 0.12$ $(\mathrm{GeV}/c)^2$.

[3]J. H. Schwarz, Phys. Rep. 8C, 269 (1973); V. Allesandrini, D. Amati, M LeBellac, and D. Olive, *ibid.* 1C, 269 (1971).

[4]G. F. Chew and A. Pignotti, Phys. Rev. Lett. 20, 1078 (1968); W. R. Frazer and C. H. Mehta, *ibid.* 23, 258 (1969).

[5]R. Lipes, G. Zweig, and W. Robertson, Phys. Rev. Lett. 22, 433 (1969); F. C. Winkelmann *et al.*, Phys. Rev. Lett. 32, 121 (1974).

[6]C. E. DeTar, Phys. Rev. D 3, 128 (1971).

[7]D. W. G. S. Leith, in *Proceedings of the XVI International Conference on High Energy Physics, Chicago-Batavia, Ill., 1972,* edited by J. D. Jackson and A. Roberts (NAL, Batavia, Ill., 1973), Vol. 3, p. 321.

[8]W. R. Frazer *et al.*, Rev. Mod. Phys. 44, 284 (1972).

[9]G. Belletini, in *High Energy Collisions—1973,* proceedings of the conference on high energy collisions, Stony Brook, 1973, edited by C. Quigg (A.I.P., New York, 1973), p. 9; S. R. Amendolia *et al.*, Phys. Lett. 48B, 359 (1974).

[10]K. Wilson, Cornell University Report No CNLS-131, 1970 (unpublished); W. Frazer, R. Peccei, S. Pinsky, and C.-I Tan, Phys. Rev. D 7, 2647 (1973); H. Harari and E. Rabinovici, Phys. Lett. 43B, 49 (1973); K. Fiałkowski and H. Miettinen, *ibid.* 43B, 61 (1973); L. Van Hove, *ibid.* 43B, 65 (1973); C. Quigg and J. D. Jackson, FNAL Report No. NAL-THY-93, 1972 (unpublished); W. Frazer, D. R. Snider, and C.-I Tan, Phys. Rev. D 8, 3180 (1973); T. L. Neff, Phys. Lett. 43B, 391 (1973); P. Pirilä and S. Pokorski, *ibid.* 43B, 502 (1973); M. Bishari and J. Koplik, *ibid.* 44B, 175 (1973); A. Capella, M.-S. Chen, M. Kugler, and R. D. Peccei, Phys. Rev. Lett. 31, 497 (1973); W. R. Frazer and D. R. Snider, Phys. Lett. 45B, 136 (1973); G. F. Chew, Phys. Rev. D 7, 934 (1973); 7, 3525 (1973); G. F. Chew, in *High Energy Collisions—1973,* proceedings of the conference on high energy collisions, Stony Brook, 1973, edited by C. Quigg (A.I.P., New York, 1973); M. Bishari, G. F. Chew, and J. Koplik, Nucl. Phys. B72, 61 (1974); M. Bishari and J. Koplik, *ibid.* B72, 93 (1974).

[11]V. N. Gribov, I. Ya. Pomeranchuk, and K. A. Ter-Martirosyan, Yad. Fiz. 2, 361 (1965) [Sov. J. Nucl. Phys. 2, 258 (1965)]; Phys. Rev. 139, B184 (1965); A. R. White, Nucl. Phys. B50, 93 (1972); B50, 130 (1972); Phys. Rev. D 10, 1236 (1974). See also I. O. Moen and W. J. Zakrzewski. Durham report, 1974 (unpublished).

[12]L. Caneschi, Phys. Rev. Lett. 23, 254 (1969); V. A. Abramovskii, O. V. Kancheli, and V. N. Gribov, in *Proceedings of the XVI International Conference on High Energy Physics, Chicago-Batavia, Ill., 1972,* edited by J. D. Jackson and A. Roberts (NAL, Batavia, Ill., 1973), Vol. 1, p. 389; I. G. Halliday and C. T. Sachrajda, Phys. Rev. D 8, 3598 (1973); A. R. White, in *Proceedings of the Eighth Rencontre de Moriond,* edited by J. Tran Thanh Van (Université de Paris-Sud, Orsay, France, 1973), Vol. II, p. 105; R. Blankenbecler, Phys. Rev. Lett. 31, 964 (1973).

[13]V. N. Gribov, Zh. Eksp. Teor. Fiz. 53, 654 (1967) [Sov. Phys.—JETP 26, 414 (1968)].

[14]I. T. Drummond, Phys. Rev. 176, 2003 (1968).

[15]V. N. Gribov and A. A. Migdal, Yad. Fiz. 8, 1002 (1968) [Sov. J. Nucl. Phys. 8, 583 (1969)]; 8, 1213 (1968) [8, 703 (1969)]; J. B. Bronzan, Phys. Rev. D 4, 1097 (1971); J. B. Bronzan and C. S. Hui, *ibid.* 5, 964 (1972); J. B. Bronzan, *ibid.* 7, 480 (1973); J. L. Cardy and A. R. White, Phys. Lett. 47B, 445 (1973).

[16]A. A. Migdal, A. M. Polyakov, and K. A. Ter-Martirosyan, Phys. Lett. 48B, 239 (1974); Moscow Report No. ITEP-102, 1973 (unpublished); H. D. I. Abarbanel and J. B. Bronzan, Phys. Rev. D 9, 2397 (1974); Phys. Lett. 48B, 345 (1974); H. D. I. Abarbanel, *ibid.* 51B, 295 (1974); R. C. Brower and J. Ellis, *ibid.* 51B, 242 (1974); R. L. Sugar and A. R. White, Phys. Rev. D 10, 4063 (1974); 10, 4074 (1974).

[17]C. E. DeTar, J. Phys. Colloque C1, 145 (1973).

[18]K. A. Ter-Martirosyan, Yad. Fiz. 10, 1047 (1969) [Sov. J. Nucl. Phys. 10, 600 (1970)]; 10, 1262 (1969) [10, 715 (1970)]; Phys. Lett. 44B, 179 (1973); V. A. Abramovskii, O. V. Kancheli, and V. N. Gribov, Ref. 12; M. Baker, in *Proceedings of the Eighth Recontre de Moriond*, edited by J. Tran Thanh Van (Université de Paris-Sud, Orsay, France, 1973), Vol. II; A. Mueller, J. Phys. Colloque C1, 307 (1973); D. Amati, Phys. Lett. 48B, 253 (1974); Uday P. Sukhatme and Carlos Pajares, Phys. Rev. D 9, 2119 (1974). For other perturbative approaches to the Pomeron, neither of the multiperipheral nor of the Reggeon-calculus variety, see J. Finkelstein and F. Zachariasen, Phys. Lett. 34B, 631 (1971); L. Caneschi and A. Schwimmer, Nucl. Phys. B44, 31 (1972); D. Amati, L. Caneschi, and M. Ciafaloni, *ibid.* B62, 173 (1973); J. Finkelstein, Phys. Rev. D 8, 4176 (1973); M. Ciafaloni and G. Marchesini, Nucl. Phys. B71, 493 (1974); CERN Report No. Ref. TH. 1835, 1973 (unpublished); D. Amati, J. Phys. Colloque C1, 129 (1973).

[19]G. F. Chew and D. R. Snider, Phys. Rev. D 1, 3453 (1970); 3, 420 (1971).

[20]H. Cheng and T. T. Wu, Phys. Rev. Lett. 24, 1456 (1970).

[21]Finkelstein, Ref. 18.

[22]H. D. I. Abarbanel, Phys. Lett. 49B, 61 (1974); J. L. Cardy, Nucl. Phys. B75, 413 (1974).

[23]G. F. Chew and D. R. Snider, Phys. Lett. 31B, 75 (1970); M. L. Goldberger, D. Silverman, and C.-I Tan, Phys. Rev. Lett. 26, 100 (1971); G. F. Chew and J. Koplik, Phys. Lett. 48B, 221 (1974).

[24]C. E. Jones, F. E. Low, S.-H. Tye, G. Veneziano, and J. E. Young, Phys. Rev. D 6, 1033 (1972); R. C. Brower and J. H. Weis, Phys. Lett. 41B, 631 (1972).

[25]R. C. Brower, C. E. DeTar, and J. H. Weis, MIT Report No. MIT-CTP-395 (unpublished); Phys. Rep. (to be published).

[26]R. J. Eden, P. V. Landshoff, D. I. Olive, and J. C. Polkinghorne, *The Analytic S-Matrix* (Cambridge University Press, Cambridge, England, 1966).

[27]V. Sudakov, Zh. Eksp. Teor. Fiz. 30, 87 (1956) [Sov. Phys.—JETP 3, 65 (1956)].

[28]A. H. Mueller, Phys. Rev. D 2, 2963 (1970).

[29]C. E. DeTar, C. E. Jones, F. E. Low, C.-I Tan, J. H. Weis, and J. E. Young, Phys. Rev. Lett. 26, 675 (1971).

[30]H. D. I. Abarbanel, Phys. Rev. D 6, 2788 (1972).

[31]S. Mandelstam, Nuovo Cimento 30, 113 (1963); 30, 1127 (1963); 30, 1148 (1963).

[32]J. H. Weis, Phys. Rev. D 4, 1777 (1971); 5, 1043 (1972); I. G. Halliday, Nucl. Phys. B33, 285 (1971); J. H. Weis, *ibid.* B71, 342 (1974).

[33]F. S. Henyey and U. P. Sukhatme, University of Michigan Report No. UM HE 74-17, 1974 (unpublished).

[34]I. J. Muzinich, F. E. Paige, T. L. Trueman, and L.-L. Wang, Phys. Rev. Lett. 28, 850 (1972).

[35]C. Pajares and D. Schiff, Nuovo Cimento Lett. 8, 237 (1973); J. N. Ng and U. P. Sukhatme, Nucl. Phys. B55, 253 (1973); N. S. Craigie and G. Preparata, Phys. Lett. 45B, 487 (1973); A. Capella and J. Kaplan, Nucl. Phys. B79, 141 (1974).

[36]P. D. B. Collins, F. D. Gault, and A. Martin, Phys. Lett. 47B, 171 (1973); Nucl. Phys. B80, 135 (1974).